SYNCHROTRON RADIATION INFRARED SPECTROMICROSCOPY: A NONINVASIVE CHEMICAL PROBE FOR MONITORING BIOGEOCHEMICAL PROCESSES

H.-Y. N. Holman[1,2] and M. C. Martin[3]

[1]Ecology Department, Earth Sciences Division,
Lawrence Berkeley National Laboratory, University of California,
Berkeley, California 94720
[2]Virtual Institute for Microbial Stress and Survival,
Lawrence Berkeley National Laboratory, University of California,
Berkeley, California 94720
[3]Advanced Light Source Division,
Lawrence Berkeley National Laboratory, University of California,
Berkeley, California 94720

A long-standing desire in biogeochemistry is to be able to examine the cycling of elements by microorganisms, as the processes are happening on surfaces of earth and environmental materials. Over the past decade, physics, engineering, and instrumentation innovations have led to the introduction of synchrotron radiation-based infrared (IR) spectromicroscopy. Spatial resolutions of less than 10 micrometers (μm) and photon energies of less than an electron volt make synchrotron IR spectromicroscopy noninvasive and useful for following the course of biogeochemical processes on complex heterogeneous surfaces of earth and environmental materials. In this chapter, we will first briefly describe the technology and then present

Advances in Agronomy, Volume 90

0065-2113/06 $35.00
DOI: 10.1016/S0065-2113(06)90003-0

several examples demonstrating its application potentials in probing and imaging biogeochemical processes.

I. INTRODUCTION

Microorganisms are important agents in the geochemical cycling of elements. For example, they can change the speciation of metal ions and organic carbons in soils and sediments by releasing complexing agents and by enzymatically catalyzing reactions (Barker and Banfield, 1996, 1998; Benzerara *et al.*, 2005; Cooper *et al.*, 2005; Edwards *et al.*, 2000, 2001; Ehrlich, 1998, 2000; Emerson and Ghiorse, 1993; Ghiorse and Hirsch, 1979; Jones *et al.*, 2003; Kalinowski *et al.*, 2000; Lajtha and Schlesinger, 1988; Lovley and Woodward, 1996; Miller *et al.*, 2004; Tebo *et al.*, 1997). They can also modify the composition of pore fluid and groundwater through controlled mineral weathering and precipitation (Andrejchuk and Klimchouk, 2001; Barker and Banfield, 1998; Bennett *et al.*, 2000; Benzerara *et al.*, 2002, 2005; Cacchio *et al.*, 2004; Cheah *et al.*, 2003; Edwards *et al.*, 2005; Ehrlich, 1994, 1998; Engel *et al.*, 2004; Goodhue *et al.*, 2005; Joeckel and Clement, 2005; Maurice *et al.*, 2001; Mcmahon and Chapelle, 1991; Renault *et al.*, 1998; Sanchez-Moral *et al.*, 2003; Spilde *et al.*, 2005; Welch *et al.*, 2002). Most importantly, they can transform many environmental pollutants to less toxic species (Aksu, 2005; Francis *et al.*, 2000, 2004; Lack *et al.*, 2002; Lovley and Phillips, 1992; Lovley *et al.*, 1993a,b; Merroun *et al.*, 2005; Neal *et al.*, 2004a; Osborne and Ehrlich, 1976; Panak *et al.*, 2002; Phillips *et al.*, 1995; Suzuki and Banfield, 2004; Watson and Ellwood, 2003; Watson *et al.*, 2000; Zouboulis and Katsoyiannis, 2005). With the discovery of diverse microbial communities thriving in every possible environment (Amend, 2004; Baker and Banfield, 2003; Balkwill and Ghiorse, 1985; Burton and Lappin-Scott, 2005; Campen *et al.*, 2003; Dees and Ghiorse, 2001; Douglas and Douglas, 2001; Edwards *et al.*, 2003; Fredrickson *et al.*, 2004; Ghiorse and Chapnick, 1983; Krumholz *et al.*, 1997; Leveille *et al.*, 2000; Macalady and Banfield, 2003; Pennisi, 2000; Schabereiter-Gurtner *et al.*, 2002; Sinclair and Ghiorse, 1989; Templeton *et al.*, 2005; Wellsbury *et al.*, 2002; Zhang and Lanoil, 2004), researchers in biogeochemistry are now increasingly focused on expanding their understanding of roles of environmental microorganisms at a more fundamental level. Many important microbial processes happen at the interface between microorganisms and earth or environmental materials. This necessitates a more comprehensive study and analysis of how microorganisms through their wide range of metabolic capabilities interact with their environments, especially at

surfaces of earth and environmental materials. This surface biogeochemistry can be highly variable at a microscopic level because of the small-scale (ranging from one micron to hundreds of microns) surface heterogeneity, which involves the distributions of clusters of mineral-inhabiting microorganisms and reactive molecules of metal oxides and organic molecules. The methodology commonly employed to study this type of heterogeneous biogeochemical phenomenon is a combination of microscopic imaging and synchrotron radiation (SR)-based X-ray spectroscopy techniques. The interested readers can read reviews (Brown and Parks, 2001; Gordon and Sturchio, 2002) and other relevant studies (Amonette *et al.*, 2003; Arnesano *et al.*, 2003; Benison *et al.*, 2004; Benzerara *et al.*, 2005; Cooper *et al.*, 2005; De Stasio *et al.*, 2001; Fein *et al.*, 2002; Foriel *et al.*, 2004; Francis *et al.*, 2004; Jones *et al.*, 2003; Jurgensen *et al.*, 2004; Khijniak *et al.*, 2005; Lack *et al.*, 2002; Li *et al.*, 2003; Lieberman *et al.*, 2003; Neal *et al.*, 2004a,b; Nesterova *et al.*, 2003; Panak *et al.*, 2002; Pickering *et al.*, 2001; Prange *et al.*, 2002a,b; Renshaw *et al.*, 2005; Saita and Maenosono, 2005; Sarret *et al.*, 2005; Suzuki *et al.*, 2003; Tebo *et al.*, 2004, 2005; Templeton *et al.*, 2005; Toner *et al.*, 2005; Twining *et al.*, 2004; Vogt *et al.*, 2003; Watson and Ellwood, 2003; Wildung *et al.*, 2004; Zouboulis and Katsoyiannis, 2005). SR-based X-ray spectromicroscopy studies have provided important and unique information about how microorganisms interact with earth and environmental materials. However, the energy range associated with SR-based X-ray spectromicroscopy techniques is between tens and thousands of electron volts (eV), which can adversely affect, harm, or even kill the microorganisms. Consequently, it has limited the use of these techniques to measuring the biogeochemical actions only at single time points.

Being able to measure real-time sequential molecular changes in a biogeochemical system, as they are happening on surfaces of earth and environmental surfaces, has been a long-standing scientific desire in biogeochemistry. The new availability of SR-based infrared (IR) sources to the scientific community in the 1990s provided this opportunity. Our group began developing an SR-based Fourier transform infrared (SR-FTIR) spectromicroscopy approach in 1998 for studying biogeochemical transformation of environmental pollutants, choosing the reduction of hexavalent chromium by living microorganisms on mineral surfaces as the initial application (Holman *et al.*, 1999). Prior to the availability of SR-based IR facilities, these type of *in vivo* and *in situ* measurements were very difficult for two reasons. First, earth materials inherently have low IR reflectivity surfaces. High-quality IR spectroscopy measurements of earth and environmental materials require a high-IR photon flux on small surface areas. Without an SR-based source, one often needs to coadd thousands to tens of thousands of spectral scans, which can be prohibitively time consuming. Second, the IR measurements of live microorganisms had been problematic.

Investigators were required to feed bacteria with a substantial quantity of deuterated substrates in order to obtain sufficient signal-to-noise spectra (Cameron *et al.*, 1983). However, deuterated substrates are known to alter activities and even produce stresses in microorganisms (Newo *et al.*, 2004; Pshenichnikova *et al.*, 2004).

There are 13 synchrotron IR spectromicroscopy facilities around the world with several more under construction or planned (see, for instance, http://www.lightsource.ca; http://www.diamond.ac.uk). Within the United States, there are four active synchrotron IR facilities with microscopy capabilities: (1) the National Synchrotron Light Source (NSLS, Brookhaven National Laboratory), (2) the Synchrotron Radiation Center (SRC, University of Wisconsin-Madison), (3) the Center for Advanced Microstructures and Devices (CAMD, Louisiana State University), and (4) the Advanced Light Source (ALS, Lawrence Berkeley National Laboratory); each has similar capabilities and uniqueness. All four are user facilities (i.e., available to qualified scientists). The first SR-FTIR spectromicroscopy experiments relevant to earth materials were the measurements of composition of clay mineral surfaces (Bantignies *et al.*, 1995), followed shortly by measurements of hydrous minerals (Lu *et al.*, 1999) and of entrapped oil–water inclusions (Guilhaumou *et al.*, 1998). The first SR-FTIR spectromicroscopy experiment relevant to cells, although not performed on bacteria, was chemical imaging of single human cells (Jamin *et al.*, 1998), bones (Miller *et al.*, 1998), and plant tissues (Wetzel *et al.*, 1998). The first SR-FTIR spectromicroscopy experiments relevant to biogeochemistry in vadose environments were the *in situ* and *in vivo* sequential measurements of reduction of hexavant chromium by a colony of basalt-inhabiting bacteria (Holman *et al.*, 1999) and of metabolization of pyrene by a colony of soil-inhabiting bacteria from a Superfund site (Holman *et al.*, 2002b). The first SR-FTIR spectromicroscopy experiments of aqueous environments was the characterization of metal–cyanobacteria sorption reactions (Yee *et al.*, 2004b).

The purposes of this chapter are to familiarize readers with SR-FTIR spectromicroscopy and to realize key issues requiring consideration prior to its application to biogeochemistry. Rather than presenting a comprehensive review of all applications of SR-FTIR spectromicroscopy, we shall focus on contents that illustrate the requirements and utility of SR-FTIR spectromicroscopy as a noninvasive molecular probe for tracking molecular changes in a biogeochemical system. The interested readers should read review articles on applications of SR-FTIR spectromicroscopy to other related areas, including ecological and agricultural sciences (Raab and Vogel, 2004), surface and environmental sciences (Hirschmugl, 2002a,b), and biology and biomedicine (Dumas *et al.*, 2004; Holman *et al.*, 2000a,b; Miller *et al.*, 2000, 2002; Wetzel *et al.*, 2005). Readers can also find

information in the reports on the applications of SR-FTIR spectromicroscopy, characterizing chemistry of fossil microorganisms (Foriel *et al.*, 2004), susceptibility of plants to mildew (Vogel *et al.*, 2002, 2004), structural–chemical features of feeds and plants (Yu, 2005a,b; Yu *et al.*, 2003, 2004), transport of pollutants in plants (Dokken *et al.*, 2005a,b,c), carbon in interplanetary dust particles (Bradley *et al.*, 2005), and microbial mineralization and silicification processes (Benning *et al.*, 2002, 2003, 2004a,b; Yee and Benning, 2002; Yee *et al.*, 2003, 2004a,b).

II. SR-FTIR SPECTROMICROSCOPY

SR-FTIR spectromicroscopy takes advantage of three existing technologies: (1) the well-known sensitivity and noninvasive nature of mid-IR spectroscopy to chemical functional groups in molecules and their conformations, (2) the convenience of a microscope to locate areas for molecular and composition analysis, and (3) the high signal-to-noise ratio provided by a noninvasive SR-based IR light source. Mid-IR spectroscopy is also a rapid, reagentless, and nondestructive analytical technique, which has a wide range of applications in biosciences, molecular or organismal. In the later section, we shall describe SR-FTIR spectromicroscopy and its issues as a biogeochemical microprobe following the background section.

A. Background

The application of SR-based IR light as a source of energy to study biogeochemical processes is an experimental effort. It is based on the principle of vibrational spectroscopy of molecules in the IR region. FTIR spectroscopy of a sample is the use of a Fourier transform interferometer to study the interaction of incoming IR light with molecules in the sample. The instrumentation for Fourier transform spectrometry includes a source of IR light, a means to measure each photon energy, an interface allowing this discreet light to be transmitted or reflected by the sample, a detector, and a data recording and analysis system. The typical measurement recorded is a spectrum of IR absorbance in the sample as a function of the wavelength of IR light (typically expressed in units of wavenumber, cm^{-1}). Atoms of a molecule vibrate with characteristic frequencies (normal modes) governed by their chemical bonds and symmetry environment. Incoming IR light will be absorbed by the molecule, if the following two criteria are met: (1) the frequency of the IR light matches exactly the frequency of the vibrational mode, and (2) the vibration causes an asymmetric change in

the charge distribution within the molecule (dipole moment). The strength of the dipole moment correlates with the strength of the absorption. IR spectroscopy is, therefore, sensitive to the presence of many chemical functional groups (structural fragments) in molecules in samples, and taken together, the set of vibration modes are unique for every molecular configuration. (More in-depth readings regarding vibrational spectroscopy of molecules and macromolecules can be found at the web site: http://infrared.als.lbl.gov/FTIRinfo.html).

IR radiation was discovered by William Herschel in 1800 during his investigations of the solar spectrum. However, the potential of using IR light energy as a source for spectroscopy was not realized until the later part of the ninteenth century. W. dew. Abney and E. R. Festing were the first researchers to successfully use IR radiation as a light source to obtain IR spectra of almost 50 organic compounds and recommended the use of IR spectroscopy as an analytical tool [Phil. Trans. Roy. Soc. London (1882). **172**, 887–918]. In 1905, William Weber Coblentz referenced this empirical evidence and demonstrated in his investigations of IR spectra that different atomic and molecular groupings absorbed specific and characteristic wavelengths. However, it is the application of Fourier transform spectroscopy in conjunction with a Michelson interferometer in 1911 by Rubens and Woods that laid the foundation of modern FTIR spectroscopy. Difficulties associated with computing Fourier transformations manually had hindered the application of the technology. Throughout the first half of the twentieth century, its applications were limited mostly to researchers in physics and astronomy, although it had found its place in the Second World War as a useful diagnostic tool in determining the concentration and purity of butadiene in synthetic rubber.

In 1949, Barer *et al.* (1949), Gore (1949), and Blout *et al.* (1949) demonstrated the potential importance of joining IR spectroscopy with microscopy to seeing microscopic structures in a sample, analyzing molecular chemistry, and relating composition with the observed microstructures (Barer, 1949, 1953, 1954; Barer and Joseph, 1954; Bird and Blout, 1952; Blout, 1953). With continued improvement in high-quality detectors and spectrometers and the rapid development in microprocessor technology, the first practical IR microspectrometer, which was conceived by Coates *et al.* (1953), became available commercially in 1978. Shortly afterwards, the innovative application of the Fast Fourier transform algorithm (Cooley and Tukey, 1965) to FTIR spectroscopy, aided by the availability of low-cost high-speed computers, has led to an explosive growth in mid-IR spectromicroscopy instrumentation primarily in the 1990s, and making it a popular analytical approach to detecting, identifying, and quantifying many molecular species mostly in biological samples.

The IR sources used in these FTIR spectromicroscopy (or microspectroscopy) instruments are thermal emission elements (or thermal globars) that produce a graybody spectrum from a filament heated to between 1000 and 2000 K. These globars can be rod-, coil-, or u-shaped, physically moderate in size (at least several millimeters), and typically radiate in all directions. As shown in Fig. 1, the FTIR bench optics collect the light, then collimate and pass it through the scanning interferometer. Next, this modulated light is directed into an IR microscope. The IR microscope objective and condenser optics are reflective and focus the IR light to a small spot on a sample. Finally, the light that the sample reflects or transmits is collected, focused onto a detector, and processed by a computer to produce an IR spectrum. The first FTIR spectromicrosocpy experiments were measurements on coals (Brenner, 1983) and polymers (Peitscher, 1986) during the first half of the 1980s. During the early 1990s, the first set of experiments performed on biological materials were on isolated human cells (Daoud *et al.*, 1988), tissue specimens (Centeno and Specht, 1992; Centeno *et al.*, 1992), and plant cells (Mccann *et al.*, 1992). The FTIR spectromicroscopy measurements of

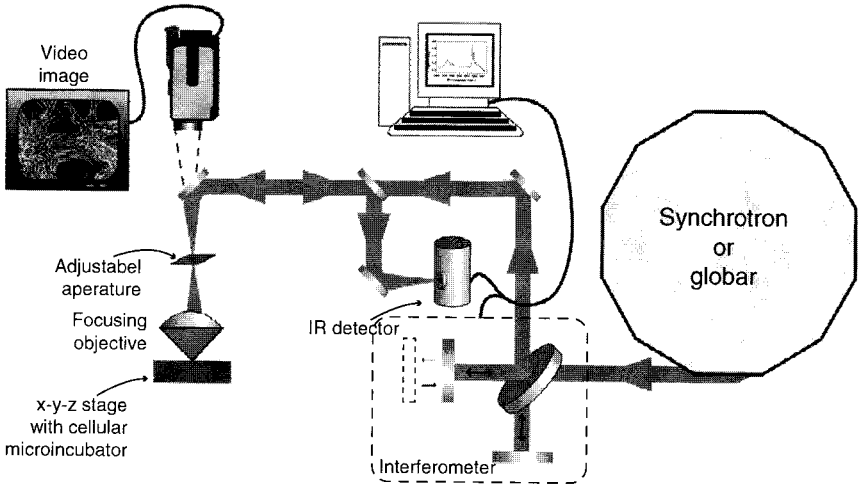

Figure 1 Schematic diagram of Fourier transform infrared (FTIR) spectromicroscopy experimental setup. Mid-IR radiation from either a synchrotron or a globar is transported to an FTIR interferometer bench. After modulation by the interferometer, an IR microscope with all-reflecting optics focuses the beam onto the sample. Microbial or biogeochemical samples can be placed inside an on-stage mini-incubator with environmental controls. The stage is computer controlled and rasters the sample in the x-y-z plane to ± 0.1 μm precision to obtain spectral maps across the sample. The light reflected from the sample is collected by the same microscope optics and sent to an IR detector. A computer performs a Fourier transform on the measured interferogram to obtain an IR spectrum. (Reproduced with permission from *Spectrosc.-Int. J.*, 2003, **17**, 139–159. IOS Press.)

bacteria were first conducted in conjunction with chemometrics to discriminate different bacterial strains (Kansiz *et al.*, 1999; Lang and Sang, 1998) almost 10 years later. The popularity of FTIR spectromicroscopy in research (as measured in terms of numbers of publications involving the applications of FTIR spectromicroscopy) soared (Fig. 2).

However, light emitted from thermal globars does not provide sufficient signal-to-noise for the detailed spectral interpretation of microbial assemblies of several to tens of microns. Such measurements were especially difficult to obtain if the microorganisms were on surfaces of earth materials with low IR reflectivities. High-quality IR spectroscopy measurements of these materials require high-IR photon flux focused to a small spot (brightness). The brightness attainable in IR spectromicroscopy is governed primarily by how point-like the source is. Thermal emission sources, for example, can be focused with an IR microscope to a spot with a 75–100-μm diameter. To measure something smaller, such as a small microbial colony on a mineral surface, one needs to use an aperture to mask away part of the incoming light, or distribute the incoming light among an array of detectors. The use of an aperture can significantly reduce the signal strength.

Our earlier work showed that the brightness (flux per unit area) attainable from a conventional thermal globar IR source is not sufficient for the use of FTIR spectromicroscopy to study biogeochemical processes on mineral surfaces without a surface treatment (Holman *et al.*, 1998). According to

the earlier discussion, it follows that one needs an IR source that acts like a true point source, that is, a source that could be focused to a diffraction-limited spot size to optimize for maximum brightness. With the f/1 optics (i.e., the primary focal ratio is *f*/1), this yields a diffraction-limited spatial resolution of approximately the wavelength of the light without loosing any signal strength. This is the benefit of using a synchrotron as an IR source.

B. Synchrotron IR Light Sources

A synchrotron is a high-energy electron storage ring, optimized for the production and collection of the intense light radiated by the electrons upon acceleration. In modern synchrotrons, electrons are first accelerated to near the speed of light and then injected into the storage ring (Fig. 3A). Electrons that travel near the speed of light are called relativistic electrons. The storage ring is designed to make the traveling electrons complete a loop via a series of bending magnets and straight sections. When the electrons encounter a magnetic field, they are deflected and emit electro-magnetic radiation—light. Typical bending magnets have a magnetic field strength of ≈1 T. This field

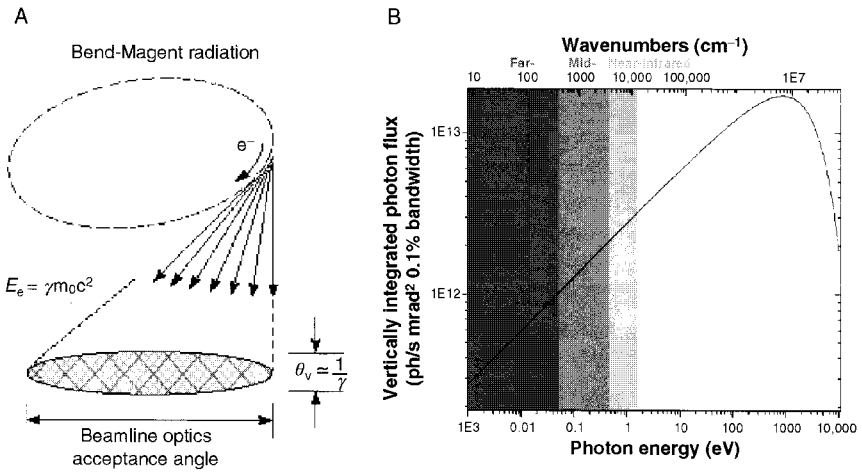

Figure 3 An overview of synchrotron radiation. (A) Guided by a series of bending magnets and straight sections, relativistic electrons inside a storage ring complete a loop. When the relativistic electrons encounter a magnetic field, they are deflected and they emit electromagnetic radiation with energy photons up to hard X-rays. (B) This so-called bending magnet spectrum extends from very low energies (far-IR) continuously to a critical energy in the soft or hard X-ray, depending on the energy of the synchrotron. The radiation pattern from relativistic electrons is such that its effective source size can be considered very close to an ideal point source. (See Color Insert.)

strength, coupled with the velocity of the electrons, determines the energies of the emitted photons. This means that higher velocities (higher energy storage rings) and/or higher magnetic fields produce higher energy photons up to hard X-rays. This so-called bending magnet spectrum (Fig. 3B) extends from very low energies (far-IR) continuously to a critical energy in the soft or hard X-ray, depending on the energy of the synchrotron. Because the radiation pattern from relativistic electrons is such that the opening angle of the emitted radiation is very small, the effective source size of the IR radiation source is dominated by diffraction, and thus can be considered as very close to an ideal point source. Interested readers are directed to an informative overview of SR by Sham and Rivers (Sham and Rivers, 2002).

As expected, in the mid-IR region — 400–4000 cm^{-1} — the effective source size for a typical synchrotron light source is dominated by diffraction (Carr *et al.*, 1995; Holman *et al.*, 2003; Reffner *et al.*, 1995, 1997). This means that for SR-FTIR spectromicroscopy the IR beam is focused visibly to a spot with a diameter of about 0.7 times the wavelength, which for the mid-IR wavelengths of 2.5–25 μm yields a spatial resolution of 1.7–17 μm (Levinson *et al.*, 2006) This is smaller than a typical microbial colony, thus, providing a spatial resolution smaller than a microbial colony with hundreds to a thousand times the brightness of conventional IR sources (Fig. 4).

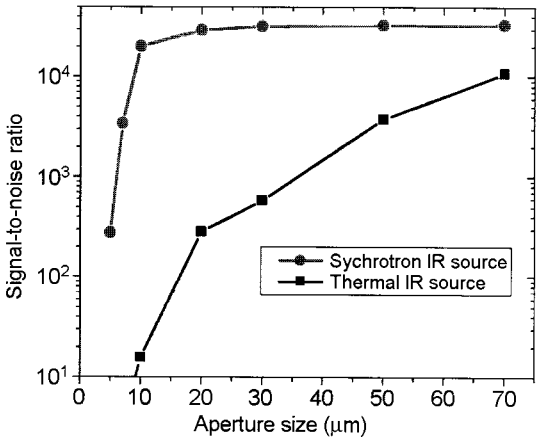

Figure 4 Comparison of measured noise around 100% reflectance for the thermal and synchrotron IR sources with different aperture size expressed in terms of signal-to-noise ratio on a log scale as a function of aperture diameters for the synchrotron and thermal IR sources. The synchrotron source extends FTIR spectromicroscopy to below 20 μm spatial resolution with a signal-to-noise advantage over conventional IR sources of at least 100. (Reproduced with permission from *Spectrosc.-Int. J.*, 2003, **17**, 139–159. IOS Press.)

To demonstrate the advantage of using a synchrotron as an IR energy source for FTIR spectromicroscopy, we describe here three studies that compare the measured signal-to-noise ratio as a function of aperture size for a conventional thermal globar IR source and the synchrotron. The first two studies were performed using a Thermo Nicolet Nexus 870 FTIR bench and a Thermo SpectraTech Contiuum IR microscope at the ALS beamline 1.4.3. The third study was performed at LURE (Laboratoire pour l'Utilisation du Rayonnement Electromagnétique, Orsay, France).

During the first experiment, we measured 100% reflection lines utilizing a gold-coated glass sample for both sources and for various aperture sizes. We used an MCT-B detector, coadded 128 scans for background and sample measurements at a spectral resolution of 4 cm^{-1} and a scanning mirror velocity of 1.8988 cm s^{-1}. The signal-to-noise value centered at 2500 cm^{-1} was obtained for both the conventional thermal source and the synchrotron source, using different aperture settings. The value was calculated by dividing the measured single beam intensity at this wavenumber by the corresponding root-mean-square (RMS) noise value. The advantage of signal-to-noise improvement is shown in Fig. 4. For the thermal globar source, the signal-to-noise level decreases significantly as the aperture diameter decreases. Signals become essentially unusable at aperture sizes below 20×20 μm^2. This is because the size of the thermal globar source, when focused to a surface, is greater than 70×70 μm^2 (Carr, 1999; Holman *et al.*, 2003; Reffner *et al.*, 1995, 1997). By reducing the aperture size, one simply reduces the total IR signal. For the synchrotron source, the signal-to-noise ratio is significantly better for almost all aperture sizes, although the ratio also begins to decrease when the aperture size is smaller than the diffraction-limited spot size. This difference is because of the focused spot size of the synchrotron source, which is diffraction limited (1.7–17 μm in diameter) (Carr, 2001; Levinson *et al.*, 2006). Consequently, its signal-to-noise ratio is only affected when the aperture size becomes less than the diffraction-limited spot size (starting with the longest wavelengths within the mid-IR region).

The second experiment compares the signal-to-noise ratio on earth materials. In Fig. 5, there is a geological example of how the high-brightness (i.e., high signal-to-noise ratio) of the synchrotron IR source makes very time consuming and difficult measurements possible. A tiny piece of ocean basalt was mounted in a diamond anvil cell to achieve extremely high pressures and the IR absorbance of the sample was measured at a pressure of 32 GPa. When using a conventional FTIR spectromicroscopy system, a 7-h signal averaging of over 60,000 scans was required to begin to detect the spectral features. With a synchrotron source, a significantly improved signal-to-noise was achieved after only 2 min of averaging 256 scans (Panero *et al.*, 2003).

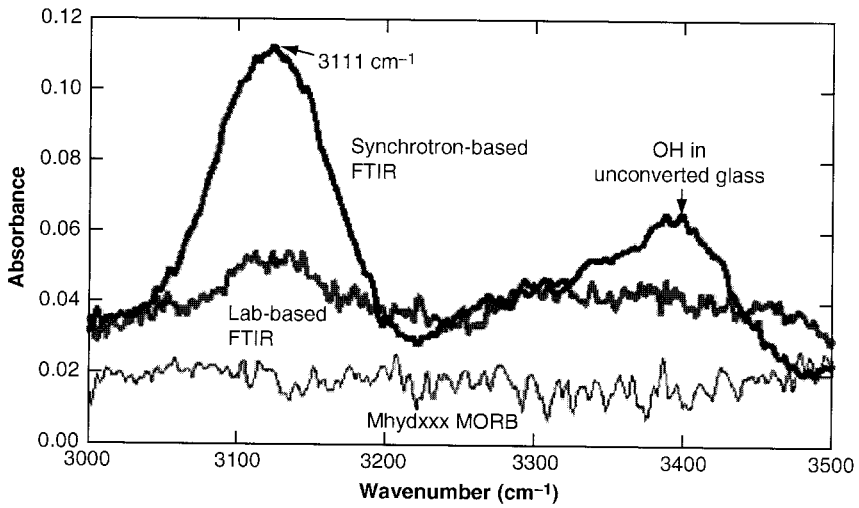

Figure 5 Spectra of a sample synthesized at 32 (±2) GPa and 2850 (±150) K, comparing results from a synchrotron-based system [black line, advanced light source (ALS) beamline 1.4.3; Nicolet Magna 760 with KBr beamsplitter and an MCT detector] to the spectrum from a lab-based system (gray line, Bruker IFS-66v using a CaF2 beamsplitter and an InSb detector). The collection time for the synchrotron-based system was about 2 min (256 scans, top) compared to about 7 h (60,000 scans, bottom) for the lab-based system. While both show a distinct peak at 3111 cm^{-1} corresponding to OH vibrations in stishovite, the synchrotron-based spectrum has a better signal-to-noise ratio, as well as better spatial resolution. There is no detectable absorption at 3450 cm^{-1}, where OH in Mg-perovskite is expected to absorb. A control experiment was performed on a dry, synthetic basalt glass starting material (sample 1114b_6); synthesis conditions were 33 (±1) GPa and 2130 (±150) K. No absorption features were found in the 3000–3500 cm^{-1} region for this sample (thin line, bottom), again collected by synchrotron FTIR (Panero *et al.*, 2003). (Reproduced with permission from *J. Geophys. Res.-Sol. Ea*, 2003, **108**, 2039–2047, American Geophysical Union.)

The third experiment compared the signal-to-noise ratio on biological materials. In Fig. 6, there are FTIR spectra from a single living cell using a $6 \times 6\ \mu m^2$ aperture (Figure courtesy of P. Dumas). In this experiment, the investigators clearly demonstrate that even with significantly longer averaging times, the signal-to-noise of the globar measurement is so poor that the data are not usable, whereas the synchrotron-based measurements show all the fine spectral structures required for detailed analysis (Dumas and Miller, 2003).

C. Synchrotron IR Spectromicroscopy of Biogeochemical Systems

The experimental evidence described earlier reveals that for studying a surface phenomenon with a spatial resolution ranging from 1.7 to 17 μm,

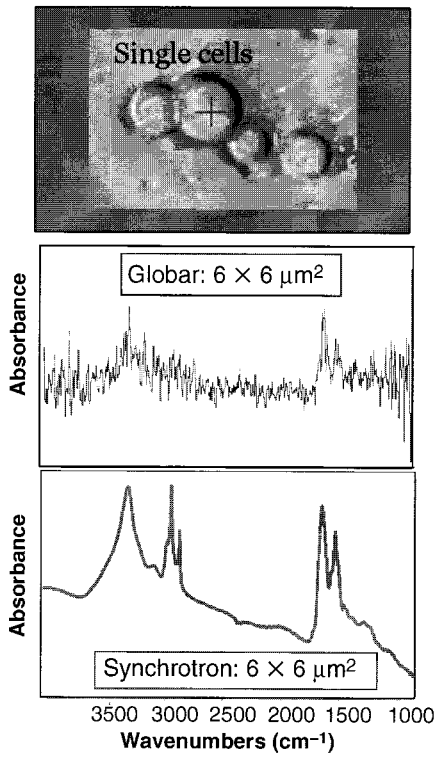

Figure 6 FTIR spectra of a single cell using a 6 × 6 μm^2 aperture, comparing results from a synchrotron-based system (red, at Laboratoire pour l'Utilisation du Rayonnement Electromagnétique, Orsay, France) to the spectrum from a lab-based system (green). The collection time for the synchrotron-based system was about 16 s (32 scans, bottom) compared to about 500 s (1000 scans, middle) for the lab-based system. These investigators clearly demonstrate that even with significantly longer averaging times, the signal-to-noise of the globar measurement is so poor that the data are not usable, whereas the synchrotron-based measurements show all the fine spectral structures required for detailed analysis. (Figure courtesy of P. Dumas.) (See Color Insert.)

the signal-to-noise ratio provided by a synchrotron IR source is up to 1000 times better than the signal-to-noise ratio provided by a thermal source. Since the SR-based IR beam does not induce any detectable side-effects in live cells (Holman *et al.*, 2002a) and has negligible sample heating effect (Martin *et al.*, 2001), SR-FTIR spectromicroscopy is clearly an ideal microprobe for a noninvasive study of heterogeneous biogeochemical processes *in vivo* and *in situ*, for example, individual microbial colonies or larger biological systems in which local biochemistry may have significant spatial variations.

However, because of the complicated nature of biogeochemical systems, one must consider the following issues carefully before applying this technology to probe the successive biogeochemical processes. First, microorganisms are exceedingly sensitive to their immediate environments. To reliably study molecular changes in a chain of biogeochemical events, SR-FTIR spectromicroscopy measurements must be made in well-controlled experiments that simulate their viability and functionality under *in situ* conditions. This is especially important since microbial cells alter earth and environmental materials mostly via their metabolic activities (Ehrlich, 1998, 2000). Such experimental conditions of biogeochemical processes are best conducted under well-controlled conditions that are similar to the *in situ* conditions. Such similarities can at least be at the appropriate temperature, pH, redox potential (Eh), nutrient, chemistry of bulk water, pore water, relative humidity, and gas composition. A good example of the importance of controlling the experimental conditions is temperature effects on microbial transformation of redox sensitive elements such as iron and sulfur. An increase in temperature could increase microbial metabolic activity and oxygen removal (Hines *et al.*, 1982), leading to a decrease in redox potential (Lyons *et al.*, 1979; Sorensen *et al.*, 1979). These changes could cause shifts in the relative importance of specific terminal electron acceptors used in bacterial respiration (Revsbech *et al.*, 1980; Sorensen *et al.*, 1979). The decrease in redox potential can also affect the chemical and physicochemical state of redox-sensitive elements. In addition to changing chemistry both in bacteria and the elements, these variations may also affect the chemistry of the overlying thin film of water through changes in diffusional fluxes and other processes. To reliably study molecular changes in this chain of biogeochemical events, SR-FTIR spectromicroscopy measurements must be made in experiments that simulate *in situ* conditions using well-controlled flow through cells with IR-transparent windows. There are several research groups developing various types of automated microfluidic incubation platforms to provide a controlled mechanism to rapidly manipulate these experimental conditions. Some of these platforms also control the thickness of the water film to allow for the IR observation of the biogeochemical processes in aqueous environments. Others have sensors to provide additional measurements of relevant physiological and geochemical parameters.

Second, a prior knowledge regarding the type of the pollutants and the pathways of their possible biogeochemical transformation is important for the successful application of SR-FTIR spectromicroscopy. For heavy metal and metalloid pollutants, they constitute the most difficult environmental problem because they cannot be destroyed once introduced into the environment. A key goal of using SR-based IR spectromicroscopy is to characterize how intrinsic microorganisms affect the speciation of these heavy metals and metalloids, which dictates the overall mobility, bioavailability,

toxicity, and other health risks in the biosphere. An appropriate SR-FTIR spectromicroscopy experiment is one that allows investigators to obtain such fundamental knowledge as the stability and mobility of the parent metal compounds, their interactions with the microorganisms, and the altered stability and mobility of the intermediate products under *in situ* and *in vivo* conditions. Our approach to this issue has been both fundamental and applied in nature. We often complement the SR-FTIR spectromicroscopy experiments with successive *in vitro* and *in vivo* studies of model systems of varying complexities to approximate membrane permeability, biotransformation, toxicity, and couple them with spectroscopic studies. In doing so, we have been able to identify, at least at a functional group level, the targets to be measured and ensure that these targets are likely to be in the biogeochemical system to be investigated.

A good example is the microbial transformation and detoxification of chromium in earth materials. Chromium is a redox-sensitive metal pollutant that enters the environment primarily from industries such as leather tanning, wood preservation, metal plating, and alloying. The two important oxidation states of chromium commonly found in environments are trivalent [Cr(III)] and hexavalent [Cr(VI)] states, which have widely contrasting mobility and bioavailability. Most Cr(VI) compounds are highly soluble in water and are readily bioavailable to ecological receptors, while most Cr(III) compounds are less water soluble and less bioavailable. Cr(VI) compounds are among the earliest chemicals to be classified as mutagens and human carcinogens (IARC, 1990; Levina *et al.*, 2003; Stern, 1982). Its genotoxic and carcinogenic effects are associated with its ability to enter cells rapidly through nonspecific transport. Intracellular biomolecules, such as polysaccharides, L-ascorbic acid, glutathione, and other reductases, readily reduce Cr(VI) species to form an array of genotoxic Cr(III) complexes and other radicals that can cause single-strand breaks and plasmid DNA nicking, in addition to a wide variety of DNA lesions and additional oxidative damage (Codd and Lay, 2001; Dillon *et al.*, 1997; Levina *et al.*, 1999; Snow, 1991; Sreedhara *et al.*, 1997; Tsou *et al.*, 1997; Voitkun *et al.*, 1998). Biogeochemical factors that can lead to the reduction of Cr(VI) to insoluble and/or nongenotoxic Cr(III) compounds in environments are very significant for reducing chromium toxicity. Many indigenous bacteria in chromium-polluted environments possess a multiplicity of survival mechanisms that can potentially transform soluble chromium to less soluble forms. Our experiments show that some Cr-resistant microorganisms immobilize and reduce Cr(VI) to stable Cr(III)-complexes extracellularly via interactions with diverse groups of biomolecules (Codd and Lay, 1999, 2001; Codd *et al.*, 1997; Gez *et al.*, 2005; Levina *et al.*, 2004) and the formation of genotoxic intermediates Cr(V)- and Cr(IV)-complexes (Kalabegishvili *et al.*, 2003; Tsibakhashvili *et al.*, 2002a). This information, in conjunction

with our earlier SR-FTIR result (Holman *et al.*, 1999), was applied to the design and execution of an additional in-depth SR-FTIR spectromicroscopy study of Cr(VI) transformation on mineral surfaces (Holman, 2004). The speciation of Cr(III) is one of the focal points in the study. There are concerns that Cr(III) [as $Cr(OH)_3$] can be reoxidized to form Cr(VI) compounds (Chinthamreddy and Reddy, 1999). However, our preliminary SR-FTIR spectromicroscopy results indicate that only a small fraction of the Cr(III) compounds is found as $Cr(OH)_3$.

Unlike heavy metals and metalloid pollutants, organic pollutants can be destroyed. Once they have entered into the biosphere, they can be degraded, metabolized, and/or mineralized by many intrinsic bacteria via one of the many possible pathways of different complexities and kinetics (da Silva *et al.*, 2003; Furukawa, 2000, 2003; Furukawa *et al.*, 1993, 2004; Hale *et al.*, 1990a,b; Kim *et al.*, 2004; Kumamaru *et al.*, 1998; Misawa *et al.*, 2002; Pothuluri *et al.*, 1995, 1998a,b, 1999; Rogers and Hale, 1987; Suenaga *et al.*, 2001, 2002). A large volume of pathway information is available at the University of Minnesota biocatalysis/biodegradation database (http://umbbd.ahc.umn.edu/). However, many of the pathways and toxicity of the intermediates are unknown. The effect of environmental factors on the microbial ability to degrade organic pollutants remains uncertain. Our approach using SR-based IR spectromicroscopy to study biodegradation of organic pollutants by intrinsic microorganisms is less fundamental but more applied in nature. Questions to be addressed include whether the microorganisms are capable of decomposing the organic pollutants, and what the geochemical factors that affect the bioavailability of the organic pollutants to the microorganisms are. For microorganisms that degrade organic pollutants via a known pathway, we would also address if the intermediates are persistent and/or harmful to ecological receptors (Holman *et al.*, 2002b).

Finally, it is important to realize that information derived from SR-FTIR spectromicroscopy is only the tip of an iceberg of information. Because of the complexity of a biogeochemical system, this information alone is not sufficient for a thorough understanding of how intrinsic microorganisms transform pollutants and what factors could alter the microbial ability to transform the pollutants. It is also not sufficient for making reliable predictions of the potential risks of these pollutants and intermediates to ecological receptors and humans. The use of multiple complementary biochemical, analytical, and imaging techniques is necessary. A good example of the use of complementary techniques is the collaborative study by researchers from the Lawrence Berkeley National Laboratory (USA) and from the Georgian Academy of Science (Republic of Georgia) of chromium reduction by basalt-inhabiting aerobes (Abuladze *et al.*, 2002; Asatiani *et al.*, 2004; Holman *et al.*, 2004; Kalabegishvili *et al.*, 2003; Tsibakhashvili *et al.*,

2002a,b, 2004). In addition to the use of SR-FTIR spectromicroscopy to track the sequential reduction of chromium, they also used sodium dodecylsulfate polyacrylamide gel electrophoresis (SDS-PAGE) to identify chromium-induced changes in cell wall protein composition (Abuladze *et al.*, 2002), capillary electrophoresis to determine the effect of cell wall proteins on the mobility of chromium through cell wall (Tsibakhashvili *et al.*, 2002a), electron spin resonance (ESR) to determine/confirm chromium speciation in bulk cells (Kalabegishvili *et al.*, 2003), and micro-X-ray fluorescence analysis (μ–XRF) and micro-x-ray absorption fine structure (μ–XAFS) imaging of Cr, Fe, and Mn distribution. Scanning electron microscopy and transmission electron microscopy were also employed (Holman *et al.*, 2004). Such synergistic use of an array of different analytical and imaging techniques has allowed these researchers to discover the unexpected accumulation and immobilization of stable and toxic chromium intermediates by microorganisms, which will have significant implications in the applications of intrinsic microorganisms to remediate Cr(VI)-polluted earth and environmental materials.

III. BIOGEOCHEMICAL PROCESSES MEASURED BY SR-FTIR SPECTROMICROSCOPY

The measurement and imaging of biogeochemical processes by means of SR-FTIR spectromicroscopy involves the use of visible light and reflecting optics to view a magnified image of the sample and to select a microscopic surface area on the sample for IR reflection–absorption spectroscopic analysis. In this section, three biogeochemical studies conducted at the ALS are highlighted, following the description of instrumentation and spectral analysis. Interested readers are directed to read applications in other related biological, biogeochemical, and environmental areas (Benning *et al.*, 2002, 2003, 2004a,b; Bonetta *et al.*, 2002; Bradley *et al.*, 2005; Dokken *et al.*, 2005a,b; Facciotti *et al.*, 2001; Foriel *et al.*, 2004; Ghosh *et al.*, 2001; Vogel *et al.*, 2002, 2004; Yee and Benning, 2002; Yee *et al.*, 2003, 2004a,b; Yu, 2005a,b; Yu *et al.*, 2003, 2004).

A. Instrumentation

The instrumentation at beamline 1.4.3 at the ALS is similar to FTIR spectromicroscopy systems that are commercially available, except that the thermal source is replaced by an IR beam from the synchrotron (Fig. 7). Additionally, the beam is also passed through a beam position-locking

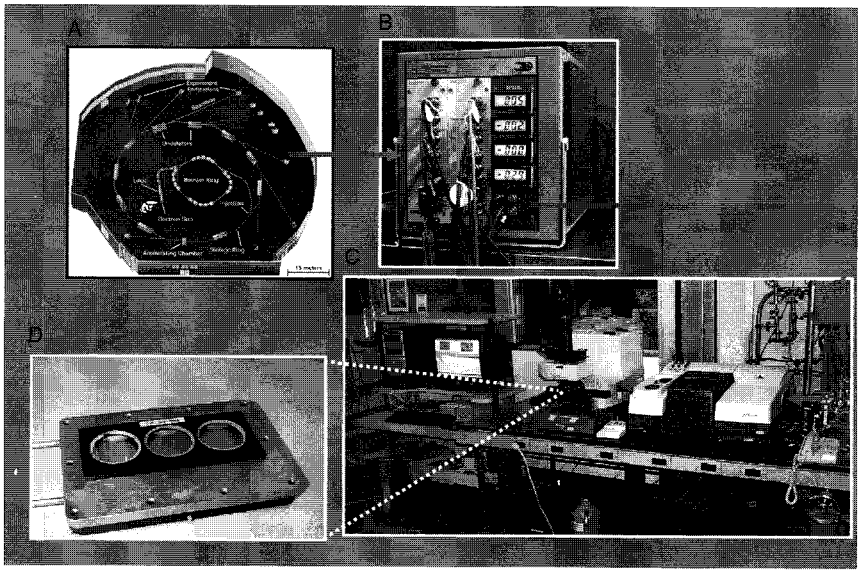

Figure 7 The beam position-locking system instrumentation at beamline 1.4.3 at the ALS. It is specifically made for probing biogeochemical processes *in situ* and *in vivo*. The beam from the synchrotron (A) is passed through the beam position-locking system (B) and then enters the commercially available FTIR spectromicroscopy system (C). During the experiment, samples are kept inside a stage mini-incubator (D). The addition of the beam-locking system is exceedingly helpful when studying biogeochemical materials that often have fine and highly heterogeneous surface features.

system (McKinney *et al.*, 2000; Scarvie *et al.*, 2004) to minimize the effect of the beam motion. Without this system, the beam tends to move on the sample during data acquisition for a variety of reasons. Such movements can be as large as several microns and cause artifacts and/or noise in the data. The addition of the beam-locking system is exceedingly helpful, when studying biogeochemical materials that often have fine and highly heterogeneous surface features.

The samples are maintained inside a mini-incubator, which is mounted on the microscope stage. The sample is positioned using a computer-controlled x-y-z stage with 0.1-μm precision allowing mapping measurements of FTIR spectra (through the incubator's ZnSe window) as a function of x- and y-position on the sample. The selection of the area is relatively subjective and relies on the geometry, color, crystallographic properties, and other material-specific features of the sample surface. Once the sample area is selected, the spectroscopic information of the selected surface area can be recorded *in situ* in a reflection mode.

B. Spectral Analysis

Because of the complexity of a biogeochemical system, one of our key efforts has been to carefully determine IR spectral features that are truly the molecular markers of the biogeochemical phenomena to be investigated. IR spectra of biomolecules in microbes (Choo-Smith *et al.*, 2001; Helm and Naumann, 1995; Helm *et al.*, 1991a,b; Kirschner *et al.*, 2001; Labischinski *et al.*, 1989; Maquelin *et al.*, 2002, 2003; Naumann *et al.*, 1982, 1988, 1996; Ngo-Thi *et al.*, 2003; Schultz and Naumann, 1991; Schultz *et al.*, 1987; Vandermei *et al.*, 1993, 1996) of many relevant minerals (Arnold and Wagner, 1988; Beran *et al.*, 1993; Collins, 1991; Delineau *et al.*, 1994; Eyring and Wadsworth, 1956; Farmer, 1974; Ha *et al.*, 1991; Keller *et al.*, 1952; Kretzschmar *et al.*, 1993; Luys *et al.*, 1982; Mielczarski *et al.*, 1993; Nguyen *et al.*, 1991; Plesko *et al.*, 1992; Povarennykh, 1978; Rossman and Aines, 1991; Salisbury *et al.*, 1991; Vilas *et al.*, 1994; White, 1971) and common environmental pollutants (Abdullah *et al.*, 2003; Bauschlicher, 1998a,b; Bauschlicher and Bakes, 2000; Bauschlicher and Langhoff, 1998; Bernstein *et al.*, 2005; Carrasco-Flores *et al.*, 2004, 2005; Chauhan *et al.*, 2004; Griffith *et al.*, 1959; Hawkins *et al.*, 1955; Hudgins and Sandford, 1998a,b,c; Hudgins *et al.*, 2000; Humphrey, 1961; Janni *et al.*, 1997; Jensen, 2004a,b; Jensen and Jensen, 2004; Li *et al.*, 2004; Ludwig *et al.*, 2000; Mattioda *et al.*, 2002; Pauzat and Ellinger, 2001, 2002; Ruiterkamp *et al.*, 2002; Seelenbinder and Brown, 2002; Todd *et al.*, 2002; Zhang *et al.*, 2005) are already well-known with specific peaks and groups of peaks that can be related to specific biochemical and chemical groups of single molecules in an ideal system. The traditional approach of spectral analysis, which is intended to identify particular compounds, involves a band-shape analysis followed by direct assignment of characteristic absorption bands in the IR spectrum. However, in a complicated and often transient biogeochemical system under *in situ* and *in vivo* conditions, these specific peaks and bands of peaks may shift, and the overall pattern may even change and deviate from the well-established features. To date, our general approach has focused on a small number of important spectral features that could be derived from a series of simplified model systems prior to the SR-FTIR spectromicroscopy experiment. For time-course experiments, we would also combine the traditional direct assignments and the difference spectroscopy approach to guide the interpretation of the absorption bands as a function of exposure time. We evaluated the intensity of each absorption band by means of the method of the most probable baseline (Lijour *et al.*, 1994). It is important to note that as the beam current of the synchrotron decreases with time between electron refills, the beam intensity decreases proportionally, which needs to be taken into account if one wants to accurately measure absorption band intensity.

We have found that rescaling the intensity of the absorption bands by means of an internal-standard equivalent approach works reliably.

C. Application Examples

With the completion of sequencing of genomes of many organisms and the continuous success in identifying gene products (proteins) and metabolic pathways, one of the central interests in biogeochemical and environmental research is to apply this wealth of information to understand and to design appropriate strategies to utilize metabolic capabilities in living microorganisms to remediate pollutants in earth and environmental materials. The success of these directions will ultimately be determined by how well one can measure without disturbing the relevant dynamic processes in a biogeochemical system, for example, the redox transformations of heavy metals by metal-reducing bacteria, or degradation of carcinogenic organic pollutants. These examples will illustrate how SR-FTIR spectromicroscopy can be a useful tool that allows one to get a step closer to achieve this important goal.

1. Reduction of Hexavalent Chromium by Basalt-Inhabiting Aerobes

Compounds containing chromium atoms can be potentially hazardous contaminants in the environment. The degree of the hazard depends on the chemical state of the chromium in the compounds in which it occurs. Chromium at its hexavalent state [Cr(VI)] is usually highly soluble in water and therefore mobile in the environment, so the contamination spreads, and it is toxic and suspected to be carcinogenic. However, chromium at its trivalent state [Cr(III)] is relatively insoluble in water and significantly less harmful. Geochemical and biogeochemical processes that convert chromium from the hexavalent to the trivalent state are potentially useful for environmental remediation. We demonstrated the use of SR-FTIR spectromicroscopy to illustrate that certain bacteria found naturally in basalt are effective agents in the "biogeochemical" transformation of chromium from the undesirable hexavalent state to the less harmful trivalent state, thereby resolving an on-going controversy about the nature of the conversion. (Holman *et al.*, 1999).

This is the first time that biogeochemical transformation of Cr(VI) by microorganisms on a mineral surface has been nondestructively monitored and studied where it occurs. Distinct and relevant IR absorption bands

(Table I) were used as chemical markers to detect the presence of microorganisms and identify different chromium species on specimen surfaces. In addition, the brightness of the IR radiation from the synchrotron IR beamline makes spatially resolved spectroscopy (spectromicroscopy) possible for imaging biogeochemical systems.

Two reduction mechanisms in polluted geological materials have previously been postulated for the reduction of Cr(VI) compounds. The biological mechanism requires the presence of microorganisms to aerobically reduce the Cr(VI). The chemical mechanism relies on metal oxides, such as Fe(II) compounds, to catalyze the Cr(VI)-reduction reaction. We conducted synchrotron FTIR spectromicroscopy experiments to distinguish the relative significance of these two mechanisms. In addition, we evaluated the effects of common organic cocontaminants, such as toluene vapor, on the biotic reduction process (Fig. 10).

For magnetite surfaces of mixed iron oxides that contain no living microorganisms, a 5-day exposure to Cr(VI) compounds resulted in statistically insignificant changes in the IR chemical markers, indicating that little catalysis of Cr(VI) reduction was occurring. On samples with living microorganisms, however, some Cr(VI) reduction was detected (Fig. 8). Moreover, when the samples with living microorganisms were incubated in dilute toluene vapor, statistically significant changes in both IR-absorption intensity and characteristic band shapes were observed for Cr(VI), as were new bands signaling the existence of intermediate Cr(V). FTIR spectromicroscopy showed that the changes in the IR absorption bands occurred at the sites of bacterial concentration. Measured images of the surface at characteristic absorption bands showed a strong correlation between peak depletion of Cr(VI) and depletion of toluene and peak concentration of biological molecules (Fig. 9).

Table I
Spectral Regions and Distinct Absorption Bands Within Each Region for Microorganisms (Including Bacteria), Cr(VI)-, Cr(V)-, and Cr(III)-Compounds, Toluene, and Catechols in Mineral/Microorganisms/Cr/Toluene System (Holman *et al.*, 1999) (Reproduced with permission from *Geomicrobiol. J.*, 1999, 16, 307–324. Copyright 1999 Taylor & Francis.)

Compounds	Spectral regions (cm^{-1})	Absorption bands (cm^{-1})
Microorganisms (protein)	1800–1500	~1650; ~1550
Cr(VI) compounds	900–800	~846; ~890
Cr(V) compounds	900–700	~830; ~764
Cr(III) compounds	850–750	~810; ~798
Toluene	800–650	~728; ~695
Catechols	800–700	~770; ~742

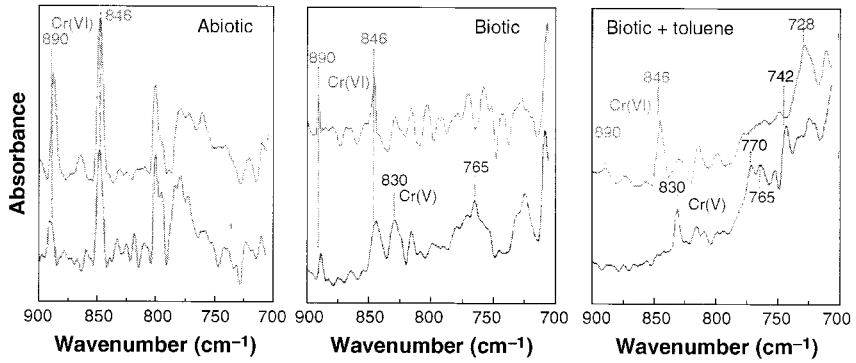

Figure 8 SR-FTIR spectra of chromate on magnetite surfaces during the 5-day experiment of (left) abiotic reduction, (middle) biotic reduction in the absence of other organic compounds, and (right) biotic reduction in the presence of toluene vapor (as a model volatile organic compound). (—) $t < 1$ day, shifted vertically for visual clarity. (—) $t = 5$ days. Although the total chromate concentration for each of the three experiments was the same, microbial-mineral surface roughness and redistribution during evaporation results in heterogeneous spatial distributions of Cr(VI) concentrations. The most relevant vibrational frequencies identified are marked: 890 and 846 cm^{-1} correspond to Cr(VI). 830 and 765 cm^{-1} correspond to Cr(V), 770 and 742 cm^{-1} are catechols, and 728 cm^{-1} is toluene. We observe that microbial reduction of Cr(VI) is the dominant mechanism in our experimental system. The microbial chromium reduction is further enhanced during the microbial degradation of the organic compound toluene (Holman *et al.*, 1999). (Reproduced with permission from *Geomicrobiol. J.*, 1999, **16**, 307–324. Copyright 1999 Taylor & Francis.) (See Color Insert.)

In a study to determine if this microbial reduction process could occur in real geological samples, composite mineral surfaces of basalt rock chips containing resident communities of microbes were exposed to solutions of Cr(VI) and toluene vapor. At the end of 4 months, FTIR spectromicroscopy showed that Cr(VI)-tolerant and Cr(VI)-reducing natural microorganisms were thriving in association with Cr(III) (Fig. 10). The reduced Cr(III) state was confirmed by XAFS spectroscopy at ALS beamline 10.3.2 (Fig. 11). The nondestructive IR spectromicroscopy studies, combined with XAFS spectroscopy and microbiological techniques, show that highly mobile and toxic Cr(VI) contaminants can be biologically reduced into less soluble, less toxic Cr(III) compounds. The FTIR method can now be expanded to examine other IR-amenable microbial/chemical contaminant systems.

2. Mycobacterial Metabolization of Pyrene in Humic Acid

Contaminants in the environment come in many forms, one of which is the relatively recalcitrant toxic organic (carbon-based) family of

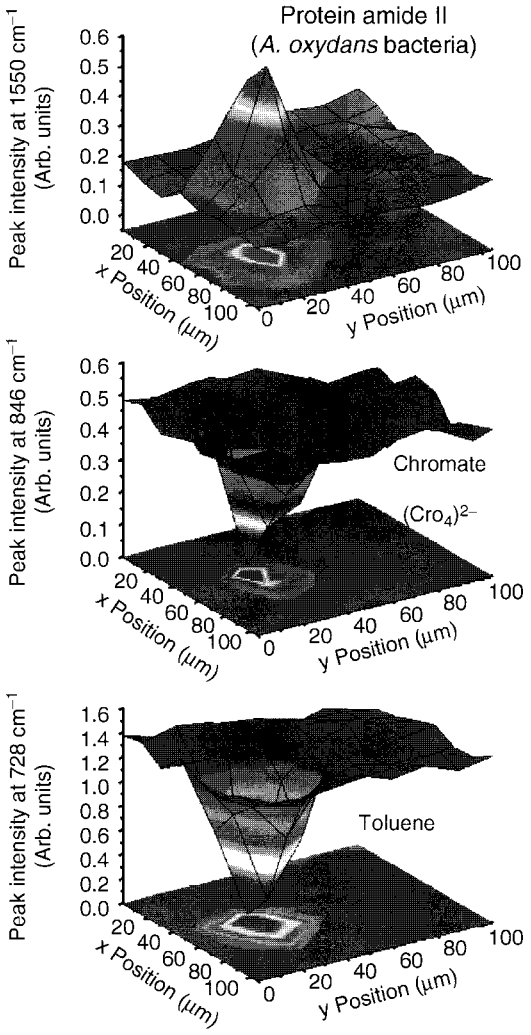

Figure 9 During the 5-day study period, *Arthrobacter oxydans* bacteria (isolated from the basalt core sample) attached themselves to magnetite surfaces. They reduced Cr(VI) while degrading toluene. SR-FTIR spectromicroscopy measurements at the end of the experiment show the spatial distribution of (top) *A. oxydans*, (middle) chromate, and (bottom) toluene, as measured by their spectral signatures (Holman *et al.*, 1999). (Reproduced with permission from *Geomicrobiol. J.*, 1999, **16**, 307–324. Copyright 1999 Taylor & Francis.) (See Color Insert.)

chemicals known as polycyclic aromatic hydrocarbons (PAHs). These include more than 100 different chemicals resulting from incomplete burning of coal, oil and gas, garbage, or other organic substances like

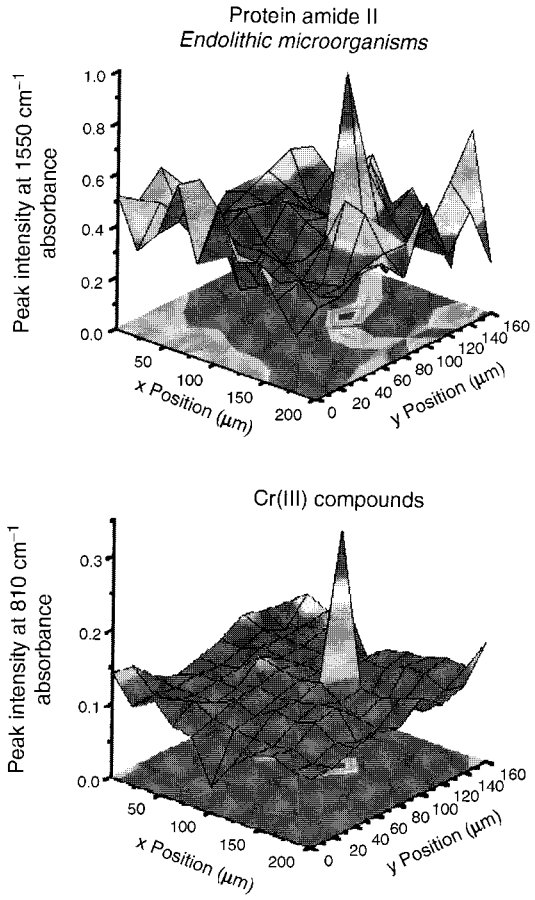

Figure 10 Distribution of indigenous endolithic microorganisms (top) and the Cr(III) compounds (bottom) as measured by SR-FTIR spectromicroscopy at the end of the 4-month Cr(VI)–microbe–basalt experiment. Only chromium-tolerant and chromium-reducing microorganisms proliferated during the study period (Holman *et al.*, 1999). (Reproduced with permission from *Geomicrobiol. J.*, 1999, **16**, 307–324. Copyright 1999 Taylor & Francis.) (See Color Insert.)

tobacco or grilled meat. Converting PAHs into nontoxic chemicals removes the hazard, but learning how to do this in an efficient and cost-effective way remains to be accomplished. Here we made use of synchrotron infrared spectromicroscopy to show that the speed of biodegradation can be dramatically increased (by almost a 100-fold) by adding a certain soil-derived organic (humic) acid along with the bacteria to a PAH spot on a mineral surface. (Holman *et al.*, 2002b).

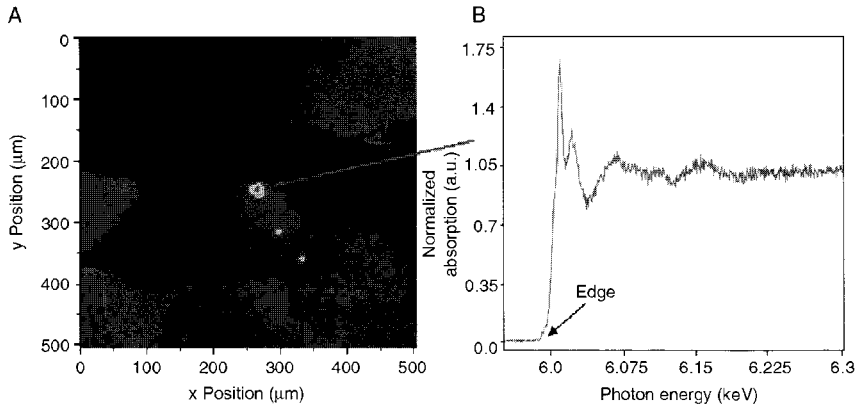

Figure 11 Confirmation of Cr (III) oxidation state by micro-X-ray analysis on the similar area of the identical sample studied by SR-FTIR (see Fig. 5). (A) Chromium elemental mapping by micro-X-ray fluorescence analysis (μ-XRF). The colors go from black (chromium concentration below detection limit) to red (high chromium concentration). (B) Average of nine micro-X-ray absorption fine structure (μ-XAFS) scans taken at the highest concentration spot shows no Cr(VI) preedge peak and is consistent with Cr(III) compounds. Each data point represents 20 s counting time. The energy increments are 0.5 eV (Holman *et al.*, 1999). (Reproduced with permission from *Geomicrobiol. J.*, 1999, **16**, 307–324. Copyright 1999 Taylor & Francis.) (See Color Insert.)

The role of humic acid (HA) in the biodegradation of toxic PAHs has been the subject of controversy, particularly in unsaturated environments. By utilizing an IR Fourier transform spectromicroscope and a very bright, nondestructive synchrotron photon source (SR-FTIR spectromicroscopy), we monitored *in situ* and over time the influence of HA on the degradation of pyrene (a model PAH) by a bacterial colony on a magnetite surface. Our results indicate that HA dramatically shortens the onset time for PAH biodegradation from 168 to 2 h. These results will have significant implications for the bioremediation of contaminated soils.

The pyrene-degrading bacterium used for this study is *Mycobacterium* sp. JLS (Fig. 12), a gram-positive, rod-shaped bacterium isolated from PAH-contaminated soil at the Libby groundwater superfund site in Libby, Montana, USA. Abiotic (no bacteria present) results (inserts in Fig. 13A and B) show that almost all of the pyrene remains on the mineral surface for the duration of the study, owing to slow removal mechanisms. After introduction of *M.* sp. JLS in the absence of HA, it took the bacteria about 168 h to produce sufficient glycolipids to solubilize pyrene. At this point, biodegradation could proceed, resulting in a rapid decrease of pyrene and a rapid increase of biomass within the next 35 h. After the pyrene was depleted, the biomass signal significantly decreased, presumably as the *M.* sp. JLS

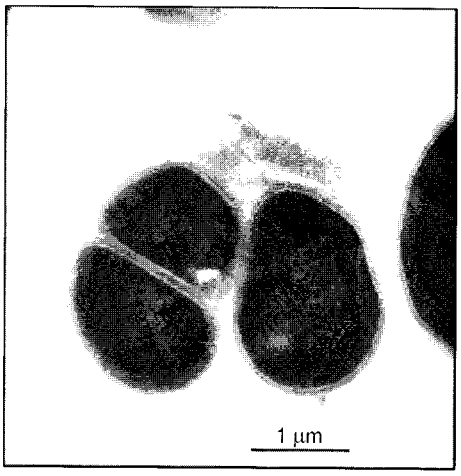

Figure 12 A transmission electron microscopy (TEM) image of the newly isolated gram-positive cocci *Mycobacterium* sp. JLS (GenBank accession no. AF387804). It appears that *M.* sp. JLS degrades polycyclic aromatic hydrocarbons, such as pyrene via a novel pathway. However, it gained biomass rapidly while degrading the compounds (Holman *et al.*, 2002b). Time-resolved analysis of spectra from SR-FTIR spectromicroscopy did not reveal fingerprints of known metabolites. This is further confirmed by follow-up mass spectrometry analysis of the sample. (Figure courtesy of W. R. Sims.)

bacteria transformed themselves into ultramicrocells, a starvation-survival strategy commonly observed among bacteria in oligotrophic environments.

In the presence of HA, pyrene biodegradation began within an hour, and the pyrene was depleted by the end of the fourth hour, with a concurrent increase of biomass (Fig. 13B). Both the degradation of pyrene and the increase of biomass corroborate the effectiveness of Elliott soil humic acid (ESHA) in radically accelerating biodegradation of pyrene. It is likely that the water-insoluble pyrene is solubilized into the cores of ESHA pseudomicelles and, therefore, becomes directly available for bacterial uptake and consumption.

Over longer times, the remaining IR absorption bands of pyrene on magnetite surfaces first showed a slight increase and subsequently a decrease. The increase is probably due to diffusion of pyrene trapped in micropores (<0.5 μm in diameter) of the magnetite and/or neighboring surfaces of higher pyrene concentration after the first wave of rapid depletion of pyrene by *M.* sp. JLS set up a diffusion gradient from the pyrene-containing micropores toward the bacterial colony. For the surface containing HA, the biomass remained almost constant over a period of more than 200 h, indicating that the flux of pyrene from the micropores was sufficient to

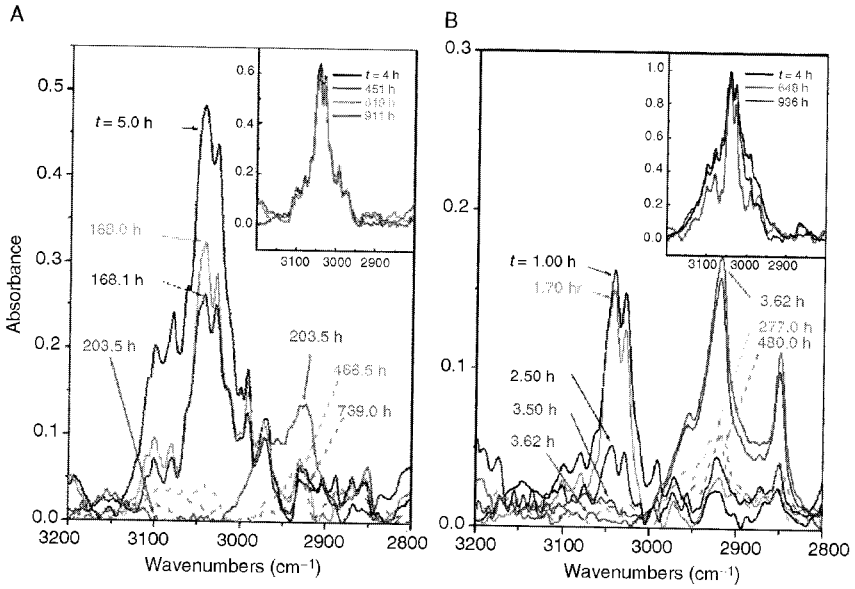

Figure 13 Time series of SR-FTIR absorption bands corresponding to pyrene and biomass formation following the degradation of pyrene by *M.* sp. JLS on magnetite surfaces. Panels A and B are from a sample free of and with ESHA. The time at which each spectrum as acquired is labeled. They show the transient behavior of pyrene doublet at 3044 and 3027 cm^{-1} and biomass IR absorption bands at 2921 and 2850 cm^{-1}. Similar behavior was observed for pyrene absorption band centered at 1185 cm^{-1}. Inserts are time series from abiotic control experiments (Holman *et al.*, 2002b). (Reproduced with permission from *Environ. Sci. Technol.*, 2002, **36**, 1276–1280. Copyright 2002 Am. Chem. Soci.) (See Color Insert.)

maintain the bacterial colony. For the surface free of HA, there is little evidence of the presence of a quasisteady state biomass (Fig. 14).

At the end of the time-resolved experiment (about 460 h), spatial distributions of pyrene, *M.* sp. JLS, and ESHA were measured by acquiring IR spectra at 5-μm intervals across the center of the bacterial colony with HA. Figure 15 shows contour maps of the spatial distribution of measured IR absorbance corresponding to *M.* sp. JLS, HA, and pyrene. The central region of the maps has a high-population density of *M.* sp. JLS and a high concentration of HA, but the pyrene in this region was completely biodegraded. Where pyrene is present without *M.* sp. JLS, there is no significant degradation.

We conclude that SR-FTIR spectromicroscopy can assess real-time interactions between multiple constituents in contaminated soils. Combined with conventional mineralization measurements, which monitor respiration through carbon dioxide production, SR-FTIR spectromicroscopy is

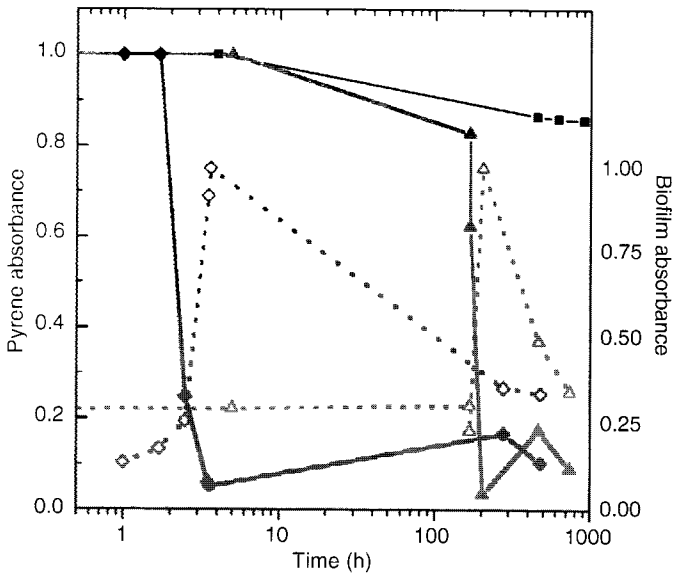

Figure 14 Summary of the SR-FTIR results showing that pyrene degradation occurs much faster when ESHA is present (note the log scale on the time axis). The pyrene absorbance was measured at 1185 cm^{-1} and biomass IR absorption band at 2921 cm^{-1}. The color scheme is black for abiotic, green for biotic without ESHA, and red for biotic with ESHA. The solid lines show the pyrene amount as a function of time for each experiment. The dotted lines show a subsequent increase in *M.* sp. JLS biomass after pyrene degradation (Holman *et al.*, 2002b). (Reproduced with permission from *Environ. Sci. Technol.*, 2002, **36**, 1276–1280. Copyright 2002 Am. Chem. Soci.) (See Color Insert.)

thus a powerful tool for evaluating bioremediation options and designing bioremediation strategies for contaminated vadose zone environments.

3. Rapid Screening for Remediation Capability of a Microbial Community

Can infrared light from a synchrotron be used to screen for metabolic activities in a living microbial community that can degrade organic pollutants? If so, it would open up possibilities for the eventual use of synchrotron infrared light in environmental diagnostics or environmental health research. The experiment summarized here is an infrared imaging of transformation of toluene by a microbial community on vesicular basalt surfaces. Our preliminary results suggest that some day

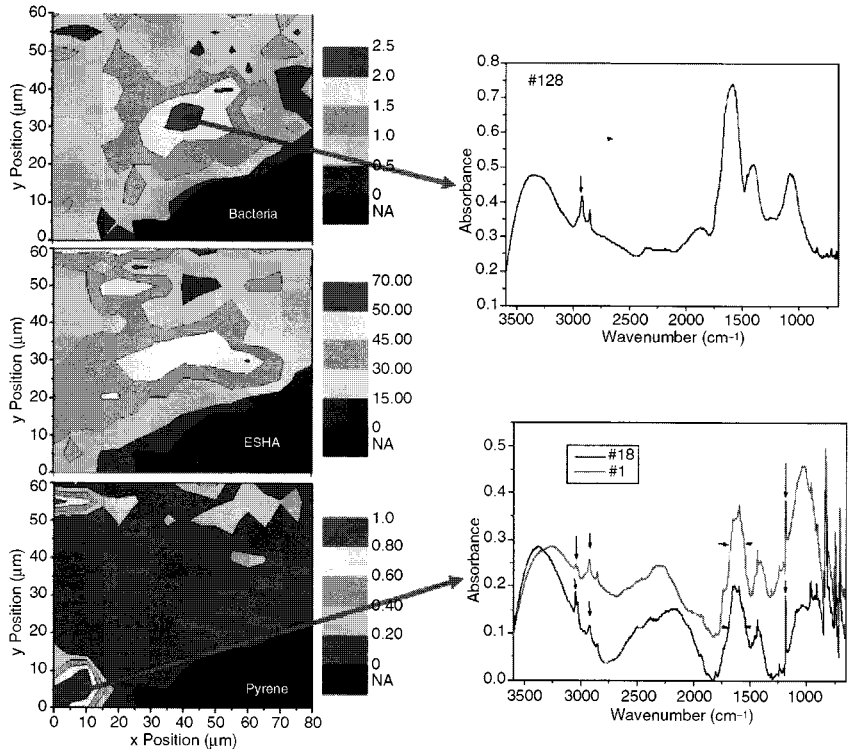

Figure 15 Contour diagrams from IR mapping obtained at the end of the experiment, showing the spatial distribution of the IR absorption peaks corresponding to (top) *M.* sp. JLS bacteria, (middle) ESHA, and (bottom) pyrene. Appropriate spectral regions were integrated for each point on the maps. The color scales for each contour plot are red for high integrated IR peak area (high concentration of the corresponding component) and blue for low peak area (low concentration); black is an out-of-focus region of the sample. The center of the map shows a region with high density of bacteria and high concentration of ESHA, where pyrene has been completely degraded (Holman *et al.*, 2002b). Note that the quality of the spectra is excellent even on such complicated surfaces of earth materials (Arrows are pointing at some of marker peaks employed in this study.) (Holman *et al.*, 2002b). (Reproduced with permission from *Environ. Sci. Technol.*, 2002, **36**, 1276–1280. Copyright 2002 Am. Chem. Soc.) (See Color Insert.)

it may be routine to study a tiny microbial colony, by using synchrotron infrared spectroscopy, and to screen for microbes and conditions that are most effective in detoxifying environmental pollutants. (Holman and Geller, 2005).

The possibility of utilizing the capability of intrinsic microorganisms to decompose and even mineralize organic pollutants has stimulated intensive interests in exploring if these biotransformation reactions actually take place on surfaces of geologic materials. Conceptual and technological

improvements in environmental microbiology have advanced our ability to partly address these issues. For example, the use of the DNA probes for specific enzymatic activities enables researchers to determine if certain genes are present in the bulk microorganisms that can initiate and sustain the desirable transformation of pollutants (Koenigsberg *et al.*, 2005). Detection of unique intermediate metabolites in site-derived samples provides evidence for the occurrence of *in situ* contaminant biotransformation. Together with microcosm experiments they globally address the questions of whether or not the bacteria interact with contaminants. However, these efforts are labor intensive and time-consuming. We are conducting a feasibility study to evaluate if SR-FTIR spectromicroscopy can be an ideal screening tool to rapidly identify microbial remedial capability on mineral surfaces.

The geological sample used was a fragment of a vesicular basalt rock from a site formerly polluted with volatile organic compounds (VOCs). The sample was exposed to 100 ppm of toluene vapor at 100% relative humidity for 5 days. Distinct and relevant IR absorption bands of toluene and its metabolites from a common degradation pathway (Fig. 16) are used to mark

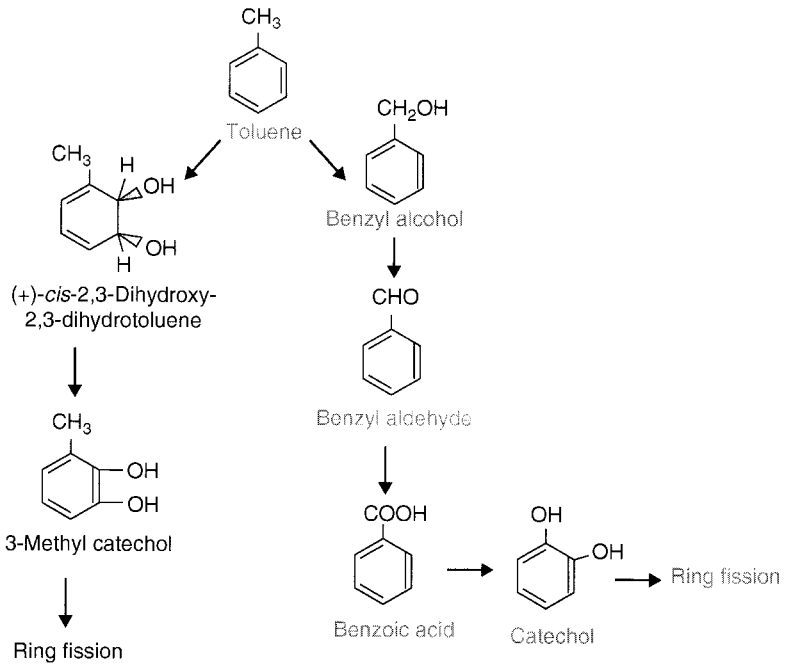

Figure 16 The possible pathway for the metabolic degradation of toluene by the intrinsic microbial communities in the earth materials. Due to matrix interference, we only tracked the marker peaks for toluene, benzyl alcohol, benzoic acid, and catechol in this study (see Table II).

the progression and capability of toluene degradation (Table II). At the end of the fifth day, chemical images from SR-FTIR spectromicroscopy showed that the native microorganisms were thriving in association with various capabilities of toluene degradation (Fig. 17). This demonstrates that the excellent spatial resolution of SR-FTIR spectromicroscopy provides a means for determining the degree to which the toxic toluene was metabolized by the microorganisms.

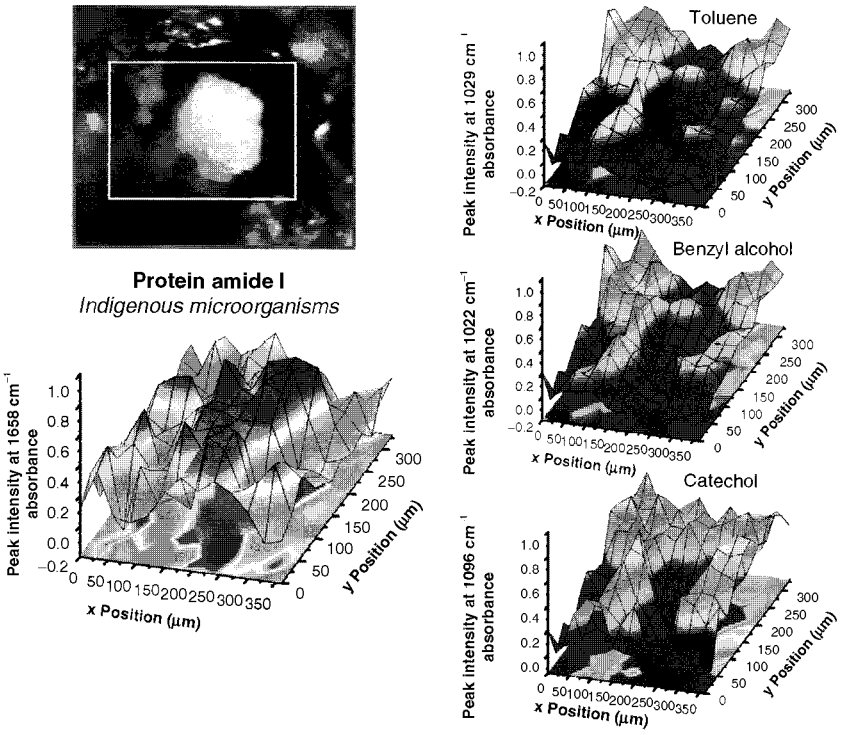

Figure 17 Chemical images from SR-FTIR spectromicroscopy showed that the native microorganisms were thriving during toluene degradation. Spectral images were rotated clockwise and tilted (relative to the bright-field micrograph) for clarity. A bright-field micrograph of microbial colonies formed on the basalt surfaces after exposure to 100-ppm toluene vapor for 5 days (left top). The spatial distribution of IR absorption peaks corresponding to (left bottom) indigenous microorganisms, (right top) toluene, and the metabolites (right middle and bottom). It appears that many native microbes metabolized nearly all the toluene immediately with some accumulation of the nontoxic metabolites benzyl alcohol and catechol. No accumulation of benzoic acid was detected. This implies that intrinsic microbial communities at the former polluted site remained efficient in detoxifying toluene (unpublished data). (See Color Insert.)

Table II
Spectral Regions and Distinct Absorption Bands Within Each Region for Microorganisms (Including Bacteria), Toluene, Benzoic Acid, and Catechols in Basalt/Microorganism/Toluene System (Holman and Geller, 2005)

Compounds	Spectral regions (cm^{-1})	Absorption bands (cm^{-1})
Microorganisms (protein)	1800–1500	~1658; ~1548
Toluene	1250–650	~1029; ~728; ~695
Benzyl alcohol	1250–650	~1200; ~1022
Benzoic acid	1250–650	~930
Catechols	1250–700	~1096; ~770; ~742

IV. FUTURE POSSIBILITIES AND REQUIREMENTS

Although SR-FTIR spectromicroscopy is an emerging analytical and imaging technology for studying biogeochemical processes *in vivo* and *in situ*, considerable experience has already been obtained in its use in evaluating microbial interactions with environmental pollutants. It seems as if only a small part of this noninvasive technology has been explored to date. For example, the quantitative capability of IR spectroscopy for accurately quantifying the transformation of metal ions or organic substrates, for defining the interrelationship between such transformation and metabolic activities, and even for measuring the chemical or activity gradient and thus the chemical fluxes across a microbial colony have not been fully utilized. Such utilities can be enhanced by a number of emerging or hoped-for advances in other relevant technologies. Improved software for the automated and accurate analysis of the spectra will make accurate quantitation easier.

Improved experimental systems are also essential. To date, the major experimental obstacles lie not in the synchrotron IR instruments themselves. Instead, they lie in two difficulties: (1) in rapidly controlling the optimum conditions for experiments before products of microbial functions are measured, and (2) in optimizing immediate data processing and interpretation. The existing techniques are relatively time consuming and labor intensive. Their fragility frequently results in major losses of sample and experimental time, and they require many steps that can take days to achieve the optimum experimental conditions.

Additionally, the future utility of the technique will also be enhanced by combining SR-FTIR spectromicroscopy with other techniques of higher specificity. For example, the most popular approach that is beneficial to

this combination appears to be the visible/IR imaging along with fluorescence microscopy. While visible imaging provides information on the physical features of the biogeochemical system and IR imaging yields global chemical information of the system, fluorescence microscopy allows one to observe localized environments (e.g., redox conditions, molecular cluster dimensions) (Kilkenny *et al.*, 2002; Rocheleau *et al.*, 2002; Zhang *et al.*, 2002) and key-dynamical processes that govern the function and structure of cells (Kahng and Shapiro, 2003; Thanbichler *et al.*, 2005; Viollier and Shapiro, 2004; Viollier *et al.*, 2002; Weijer, 2003). The fluorescent probes can be endogenous molecules such as NAD(P)H (Latouche *et al.*, 2000; Piston and Knobel, 1999; Simon *et al.*, 1996), genetically encoded specific fluorescent proteins (Orser *et al.*, 1995; Vandyk *et al.*, 1995), or passive markers of specific fluorescent molecules/dyes (Haugland, 2002). By establishing an associative analysis that links the genetically encoded molecules and marked cellular events from fluorescence microscopy to the global chemical information derived from SR-FTIR spectromicrosocpy, one can truly expand the existing understanding of biogeochemical capabilities in living microbes and developing biotechnologies for utilizing such capabilities for the benefit of environmental management.

ACKNOWLEDGMENTS

We would like to thank Dr. Eleanor Wozei for her careful review of the chapter. This work was performed with support by the Directors of the Office of Science, Office of Biological and Environmental Research, Medical Science Division, Office of National Petroleum Technology Program, Office of Science, Basic Energy Sciences, Materials Science Division of the US Department of Energy under Contract No. DE-AC03–76SF00098, and the Army Corps of Engineers of the US Department of Defense.

REFERENCES

Abdullah, H. H., Kubba, R. M., and Shanshal, M. (2003). Vibration frequencies shifts of naphthalene and anthracene as caused by different molecular charges. *Z. Naturforsch. A* **58**, 645–655.

Abuladze, M. K., Asatiani, N. V., Bakradze, N. G., Kartvelishvili, T. M., Holman, H.-Y. N., Kalabegishvili, T. L., Mosulishvili, L. M., Rcheulishvili, A. N., Sapojnikova, N. A., and Tsibakhashvili, N. Y. (2002). Effect of chromium action on the protein composition of Arthrobacter oxydans. *Fresen. Environ. Bull.* **11**, 562–567.

Aksu, Z. (2005). Application of biosorption for the removal of organic pollutants: A review. *Process Biochem.* **40**, 997–1026.

Amend, J. (2004). Geomicrobiology and genomes. *Geotimes* **49**, 40–41.

Amonette, J. E., Heald, S. M., and Russell, C. K. (2003). Imaging the heterogeneity of mineral surface reactivity using Ag(I) and synchrotron X-ray microscopy. *Phys. Chem. Miner.* **30**, 559–569.

Andrejchuk, V. N., and Klimchouk, A. B. (2001). Geomicrobiology and redox geochemistry of the karstified Miocene gypsum aquifer, western Ukraine: The study from Zoloushka Cave. *Geomicrobiol. J.* **18**, 275–295.

Arnesano, F., Banci, L., Bertini, I., Mangani, S., and Thompsett, A. R. (2003). A redox switch in CopC: An intriguing copper trafficking protein that binds copper(I) and copper(II) at different sites. *Proc. Natl. Acad. Sci. USA* **100**, 3814–3819.

Arnold, G., and Wagner, C. (1988). Grain-size influence on the mid-infrared spectra of the minerals. *Earth Moon Planets* **41**, 163–171.

Asatiani, N. V., Abuladze, M. K., Kartvelishvili, T. M., Bakradze, N. G., Sapojnikova, N. A., Tsibakhashvili, N. Y., Tabatadze, L. V., Lejava, L. V., Asanishvili, L. L., and Holman, H.-Y. (2004). Effect of chromium(VI) action on *Arthrobacter oxydans*. *Curr. Microbiol.* **49**, 321–326.

Baker, B. J., and Banfield, J. F. (2003). Microbial communities in acid mine drainage. *FEMS Microbiol. Ecol.* **44**, 139–152.

Balkwill, D. L., and Ghiorse, W. C. (1985). Characterization of subsurface bacteria associated with 2 shallow aquifers in Oklahoma. *Appl. Environ. Microb.* **50**, 580–588.

Bantignies, J. L., Moulin, C. C. D., Dexpert, H., Flank, A. M., and Williams, G. (1995). Asphaltene adsorption on kaolinite—characterization by infrared microspectroscopy and X-Ray-absorption spectroscopy. *CR Acad. Sci. II* **320**, 699–706.

Barer, G. R. (1954). Quantitative measurements on spreading phenomena in skin. *Brit. J. Pharm. Chemoth.* **9**, 346–351.

Barer, R. (1949). The reflecting microscope in anatomical research. *J. Anat.* **83**, 73–74.

Barer, R. (1953). Determination of dry mass, thickness, solid and water concentration in living cells. *Nature* **172**, 1097–1098.

Barer, R., and Joseph, S. (1954). Refractometry of living cells.1. Basic principles. *Q. J. Microsc. Sci.* **95**, 399–423.

Barer, R., Cole, A. R. H., and Thompson, H. W. (1949). Infra-red spectroscopy with the reflecting microscope in physics, chemistry and biology. *Nature* **163**, 198–201.

Barker, W. W., and Banfield, J. F. (1996). Biologically versus inorganically mediated weathering reactions: Relationships between minerals and extracellular microbial polymers in lithobiontic communities. *Chem. Geol.* **132**, 55–69.

Barker, W. W., and Banfield, J. F. (1998). Zones of chemical and physical interaction at interfaces between microbial communities and minerals: A model. *Geomicrobiol. J.* **15**, 223–244.

Bauschlicher, C. W. (1998a). Infrared spectra of polycyclic aromatic hydrocarbons: Nitrogen substitution. *Chem. Phys.* **234**, 87–94.

Bauschlicher, C. W. (1998b). Infrared spectra of polycyclic aromatic hydrocarbons: Oxygen substitution. *Chem. Phys.* **233**, 29–34.

Bauschlicher, C. W., and Bakes, E. L. O. (2000). Infrared spectra of polycyclic aromatic hydrocarbons (PAHs). *Chem. Phys.* **262**, 285–291.

Bauschlicher, C. W., and Langhoff, S. R. (1998). Infrared spectra of polycyclic aromatic hydrocarbons: Methyl substitution and loss of H. *Chem. Phys.* **234**, 79–86.

Benison, G. C., Di Lello, P., Shokes, J. E., Cosper, N. J., Scott, R. A., Legault, P., and Omichinski, J. G. (2004). A stable mercury-containing complex of the organomercurial lyase MerB: Catalysis, product release, and direct transfer to MerA. *Biochemistry-US* **43**, 8333–8345.

Bennett, P. C., Hiebert, F. K., and Rogers, J. R. (2000). Microbial control of mineral-groundwater equilibria: Macroscale to microscale. *Hydrogeol. J.* **8**, 47–62.

Benning, L. G., Yee, N., Phoenix, V., and Konhauser, K. O. (2002). The *in situ* molecular characterisation of a biomineralization process: A synchrotron infrared study. *Geochim. Cosmochim. Acta* **66**(Suppl. 1), A68.

Benning, L. G., Phoenix, V., Yee, N., and Hammer, O. (2003). Bacterial-silica interactions: Affinity or fate? *Abst. Pap. Am. Chem. S.* **226**, U590.

Benning, L. G., Phoenix, V. R., Yee, N., and Konhauser, K. O. (2004a). The dynamics of cyanobacterial silicification: An infrared micro-spectroscopic investigation. *Geochim. Cosmochim. Acta* **68**, 743–757.

Benning, L. G., Phoenix, V. R., Yee, N., and Tobin, M. J. (2004b). Molecular characterization of cyanobacterial silicification using synchrotron infrared micro-spectroscopy. *Geochim. Cosmochim. Acta* **68**, 729–741.

Benzerara, K., Chapon, V., Heulin, T., Guyot, F., Menguy, N., Skouri, F., and Barakat, M. (2002). Geomicrobiology of carbonate precipitations at the surface of pyroxenes in an aridic soil. *Geochim. Cosmochim. Acta* **66**, A69.

Benzerara, K., Yoon, T. H., Menguy, N., Tyliszczak, T., and Brown, G. E. (2005). Nanoscale environments associated with bioweathering of a Mg-Fe-pyroxene. *Proc. Natl. Acad. Sci. USA* **102**, 979–982.

Beran, A., Langer, K., and Andrut, M. (1993). Single-crystal infrared-spectra in the range of Oh fundamentals of paragenetic garnet, omphacite and kyanite in an eklogitic mantle xenolith. *Miner. Petrol.* **48**, 257–268.

Bernstein, M. P., Mattioda, A. L., Sandford, S. A., and Hudgins, D. M. (2005). Laboratory infrared spectra of polycyclic aromatic nitrogen heterocycles: Quinoline and phenanthridine in solid argon and H2O. *Astrophys. J.* **626**, 909–918.

Bird, G. R., and Blout, E. R. (1952). Infrared microspectroscopy of biologic materials. *Lab. Invest.* **1**, 266–272.

Blout, E. R. (1953). Infrared microspectroscopy—instrumentation and some biological applications. *Trans. N. Y. Acad. Sci.* **15**, 280–281.

Blout, E. R., Bird, G. R., and Grey, D. S. (1949). Infrared microspectroscopy. *Anal. Chem.* **21**, 1585.

Bonetta, D. T., Facette, M., Raab, T. K., and Somerville, C. R. (2002). Genetic dissection of plant cell-wall biosynthesis. *Biochem. Soc. Trans.* **30**, 298–301.

Bradley, J., Dai, Z. R., Erni, R., Browning, N., Graham, G., Weber, P., Smith, J., Hutcheon, I., Ishii, H., Bajt, S., Floss, C., Stadermann, F., *et al.* (2005). An astronomical 2175 angstrom feature in interplanetary dust particles. *Science* **307**, 244–247.

Brenner, D. (1983). Infrared microspectroscopy of coals. *P. Soc. Photo-opt. Inst.* **411**, 8–12.

Brown, G. E., and Parks, G. A. (2001). Sorption of trace elements on mineral surfaces: Modern perspectives from spectroscopic studies, and comments on sorption in the marine environment. *Int. Geol. Rev.* **43**, 963–1073.

Burton, S. K., and Lappin-Scott, H. M. (2005). Geomicrobiology, the hidden depths of the biosphere. *Trends Microbiol.* **13**, 401.

Cacchio, P., Contento, R., Ercole, C., Cappuccio, G., Martinez, M. P., and Lepidi, A. (2004). Involvement of microorganisms in the formation of carbonate speleothems in the Cervo Cave (L'Aquila-Italy). *Geomicrobiol. J.* **21**, 497–509.

Cameron, D. G., Martin, A., and Mantsch, H. H. (1983). Membrane isolation alters the gel to liquid-crystal transition of Acholeplasma-laidlawii-B. *Science* **219**, 180–182.

Campen, R. K., Sowers, T., and Alley, R. B. (2003). Evidence of microbial consortia metabolizing within a low-latitude mountain glacier. *Geology* **31**, 231–234.

Carr, G. L. (1999). High-resolution microspectroscopy and sub-nanosecond time-resolved spectroscopy with the synchrotron infrared source. *Vib. Spectrosc.* **19**, 53–60.

Carr, G. L. (2001). Resolution limits for infrared microspectroscopy explored with synchrotron radiation. *Rev. Sci. Instrum.* **72**(3), 1613–1619.

Carr, G. L., Reffner, J. A., and Williams, G. P. (1995). Performance of an infrared microspectrometer at the NSLS. *Rev. Sci. Instrum.* **66**, 1490–1492.

Carrasco-Flores, E. A., Clavijo, R. E., Campos-Vallette, M. M., and Aroca, R. F. (2004). Vibrational spectra and surface-enhanced vibrational spectra of 1-nitropyrene. *Appl. Spectrosc.* **58**, 555–561.

Carrasco-Flores, E. A., Clavijo, R. E., Campos-Vallette, M. M., and Aroca, R. F. (2005). Vibrational and surface-enhanced vibrational spectra of 6-nitrochrysene. *Spectrochim. Acta A* **61**, 509–514.

Centeno, J. A., and Specht, C. S. (1992). Infrared microspectroscopy of extracellular-matrix proteins in macular and stroma scar of the cornea. *FASEB J.* **6**, A478.

Centeno, J. A., Kalasinsky, V. F., Johnson, F. B., Vinh, T. N., and Oleary, T. J. (1992). Fourier-transform infrared microscopic identification of foreign materials in tissue-sections. *Lab. Invest.* **66**, 123–131.

Chauhan, H. P. S., Shaik, N. M., and Kori, K. (2004). Synthesis and characterization of some toluene-3,4-dithiolatobismuth(III) alkyl dithiocarbonates. *Synth. React. Inorg. Me.* **34**, 323–333.

Cheah, S. F., Kraemer, S. M., Cervini-Silva, J., and Sposito, G. (2003). Steady-state dissolution kinetics of goethite in the presence of desferrioxamine B and oxalate ligands: Implications for the microbial acquisition of iron. *Chem. Geol.* **198**, 63–75.

Chinthamreddy, S., and Reddy, K. R. (1999). Oxidation and mobility of trivalent chromium in manganese-enriched clays during electrokinetic remediation. *J. Soil Contam.* **8**, 197–216.

Choo-Smith, L. P., Maquelin, K., van Vreeswijk, T., Bruining, H. A., Puppels, G. J., Thi, N. A. G., Kirschner, C., Naumann, D., Ami, D., Villa, A. M., Orsini, F., Doglia, S. M., *et al.* (2001). Investigating microbial (micro)colony heterogeneity by vibrational spectroscopy. *Appl. Environ. Microbiol.* **67**, 1461–1469.

Coates, V. J., Offner, A., and Siegler, E. H. (1953). Design and performance of an infrared microscope attachment. *J. Opt. Soc. Am.* **43**, 984–989.

Codd, R., and Lay, P. A. (1999). Competition between 1,2-diol and 2-hydroxy acid coordination in Cr(V)-quinic acid complexes: Implications for stabilization of Cr(V) intermediates of relevance to Cr(VI)-induced carcinogenesis. *J. Am. Chem. Soc.* **121**, 7864–7876.

Codd, R., and Lay, P. A. (2001). Chromium(V)-sialic (neuraminic) acid species are formed from mixtures of chromium(VI) and saliva. *J. Am. Chem. Soc.* **123**, 11799–11800.

Codd, R., Lay, P. A., and Levina, A. (1997). Stability and ligand exchange reactions of chromium(IV) carboxylato complexes in aqueous solutions. *Inorg. Chem.* **36**, 5440–5448.

Collins, A. H. (1991). Thermal infrared-spectra and images of altered volcanic-rocks in the Virginia Range, Nevada. *Int. J. Remote Sens.* **12**, 1559–1574.

Cooley, J. W., and Tukey, J. W. (1965). An algorithm for machine calculation of complex Fourier series. *Math. Comput.* **19**, 297–301.

Cooper, D. C., Neal, A. L., Kukkadapu, R. K., Brewe, D., Coby, A., and Picardal, F. W. (2005). Effects of sediment iron mineral composition on microbially mediated changes in divalent metal speciation: Importance of ferrihydrite. *Geochim. Cosmochim. Acta* **69**, 1739–1754.

da Silva, M., Cerniglia, C. E., Pothuluri, J. V., Canhos, V. P., and Esposito, E. (2003). Screening filamentous fungi isolated from estuarine sediments for the ability to oxidize polycyclic aromatic hydrocarbons. *World J. Microbiol. Biot.* **19**, 399–405.

Daoud, C., Joly, P., Angiboust, J. F., and Manfait, M. (1988). Fourier-transform infrared microspectroscopy of isolated cells. *Ann. Biol. Clin.-Paris* **46**, 577.

De Stasio, G., Gilbert, B., Frazer, B. H., Nealson, K. H., Conrad, P. G., Livi, V., Labrenz, M., and Banfield, J. F. (2001). The multidisciplinarity of spectromicroscopy: From geomicrobiology to archaeology. *J. Electron Spectrosc.* **114**, 997–1003.

Dees, P. M., and Ghiorse, W. C. (2001). Microbial diversity in hot synthetic compost as revealed by PCR-amplified rRNA sequences from cultivated isolates and extracted DNA. *FEMS Microbiol. Ecol.* **35**, 207–216.

Delineau, T., Allard, T., Muller, J. P., Barres, O., Yvon, J., and Cases, J. M. (1994). FTIR reflectance vs EPR studies of structural iron in kaolinites. *Clay Clay Miner.* **42**, 308–320.

Dillon, C. T., Lay, P. A., Cholewa, M., Legge, G. J. F., Bonin, A. M., Collins, T. J., Kostka, K. L., and SheaMcCarthy, G. (1997). Microprobe X-ray absorption spectroscopic determination of the oxidation state of intracellular chromium following exposure of V79 Chinese hamster lung cells to genotoxic chromium complexes. *Chem. Res. Toxicol.* **10**, 533–535.

Dokken, K. M., Davis, L. C., Erickson, L. E., Castro-Diaz, S., and Marinkovic, N. S. (2005a). Synchrotron fourier transform infrared micro spectroscopy: A new tool to monitor the fate of organic contaminants in plants. *Microchem. J.* **81**, 86–91.

Dokken, K. M., Davis, L. C., and Marinkovic, N. S. (2005b). Use of infrared microspectroscopy in plant growth and development. *Appl. Spectrosc. Rev.* **40**, 301–326.

Dokken, K. M., Davis, L. C., and Marinkovic, N. S. (2005c). Using SR-IMS to study the fate and transport of organic contaminants in plants. *Spectroscopy* **20**, 14–18.

Douglas, S., and Douglas, D. D. (2001). Structural and geomicrobiological characteristics of a microbial community from a cold sulfide spring. *Geomicrobiol J.* **18**, 401–422.

Dumas, P., and Miller, L. (2003). The use of synchrotron infrared microspectroscopy in biological and biomedical investigations. *Vib. Spectrosc.* **32**, 3–21.

Dumas, P., Jamin, N., Teillaud, J. L., Miller, L. M., and Beccard, B. (2004). Imaging capabilities of synchrotron infrared microspectroscopy. *Faraday Discuss.* **126**, 289–302.

Edwards, K. J., Bond, P. L., Druschel, G. K., McGuire, M. M., Hamers, R. J., and Banfield, J. F. (2000). Geochemical and biological aspects of sulfide mineral dissolution: Lessons from Iron Mountain, California. *Chem. Geol.* **169**, 383–397.

Edwards, K. J., Hu, B., Hamers, R. J., and Banfield, J. F. (2001). A new look at microbial leaching patterns on sulfide minerals. *FEMs Microbiol. Ecol.* **34**, 197–206.

Edwards, K. J., Bach, W., and Rogers, D. R. (2003). Geomicrobiology of the ocean crust: A role for chemoautotrophic Fe-bacteria. *Biol. Bull.* **204**, 180–185.

Edwards, K. J., Bach, W., and McCollom, T. M. (2005). Geomicrobiology in oceanography: Microbe-mineral interactions at and below the seafloor. *Trends Microbiol.* **13**, 449–456.

Ehrlich, H. L. (1994). Special issue: Breakthroughs in karst geomicrobiology and redox geochemistry—foreword. *Geomicrobiol. J.* **12**, 135.

Ehrlich, H. L. (1998). Geomicrobiology: Its significance for geology. *Earth-sci. Rev.* **45**, 45–60.

Ehrlich, H. L. (2000). Geomicrobiology. *Geotimes* **45**, 34–37.

Emerson, D., and Ghiorse, W. C. (1993). Ultrastructure and chemical-composition of the sheath of *Leptothrix discophora* Sp-6. *J. Bacteriol.* **175**, 7808–7818.

Engel, A. S., Stern, L. A., and Bennett, P. C. (2004). Microbial contributions to cave formation: New insights into sulfuric acid speleogenesis. *Geology* **32**, 369–372.

Eyring, E. M., and Wadsworth, M. E. (1956). Differential infrared spectra of adsorbed monolayers-normal-hexanethiol on Zn minerals. *T. Am. I. Min. Met. Eng.* **205**, 531–535.

Facciotti, M. T., Rouhani, S., Burkard, F. T., Betancourt, F. M., Downing, K. H., Rose, R. B., McDermott, G., and Glaeser, R. M. (2001). Structure of an early intermediate in the M-state phase of the bacteriorhodopsin photocycle. *Biophys. J.* **81**, 3442–3455.

Farmer, V. C. (Ed.) (1974). "The Infrared Spectra of Minerals."Mineralogical Society, London.

Fein, J. B., Fowle, D. A., Cahill, J., Kemner, K., Boyanov, M., and Bunker, B. (2002). Nonmetabolic reduction of Cr(VI) by bacterial surfaces under nutrient-absent conditions. *Geomicrobiol. J.* **19**, 369–382.

Foriel, J., Philippot, P., Susini, J., Dumas, P., Somogyi, A., Salome, M., Khodja, H., Menez, M., Fouquet, Y., Moreira, D., and Lopez-Garcia, P. (2004). High-resolution imaging of sulfur oxidation states, trace elements, and organic molecules distribution in individual microfossils and contemporary microbial filaments. *Geochim. Cosmochim. Acta* **68**, 1561–1569.

Francis, A. J., Dodge, C. J., Gillow, J. B., and Papenguth, H. W. (2000). Biotransformation of uranium compounds in high ionic strength brine by a halophilic bacterium under denitrifying conditions. *Environ. Sci. Technol.* **34**, 2311–2317.

Francis, A. J., Gillow, J. B., Dodge, C. J., Harris, R., Beveridge, T. J., and Papenguth, H. W. (2004). Uranium association with halophilic and non-halophilic bacteria and archaea. *Radiochim. Acta* **92**, 481–488.

Fredrickson, J. K., Zachara, J. M., Balkwill, D. L., Kennedy, D., Li, S. M. W., Kostandarithes, H. M., Daly, M. J., Romine, M. F., and Brockman, F. J. (2004). Geomicrobiology of high-level nuclear waste-contaminated vadose sediments at the Hanford site, Washington State. *Appl. Environ. Microbiol.* **70**, 4230–4241.

Furukawa, K. (2000). Biochemical and genetic bases of microbial degradation of polychlorinated biphenyls (PCBs). *J. Gen. Appl. Microbiol.* **46**, 283–296.

Furukawa, K. (2003). "Super bugs" for bioremediation. *Trends Biotechnol.* **21**, 187–190.

Furukawa, K., Hirose, J., Suyama, A., Zaiki, T., and Hayashida, S. (1993). Gene components responsible for discrete substrate-specificity in the metabolism of biphenyl (Bph operon) and toluene (Tod operon). *J. Bacteriol.* **175**, 5224–5232.

Furukawa, K., Suenaga, H., and Goto, M. (2004). Biphenyl dioxygenases: Functional versatilities and directed evolution. *J. Bacteriol.* **186**, 5189–5196.

Gez, S., Luxenhofer, R., Levina, A., Codd, R., and Lay, P. A. (2005). Chromium(V) complexes of hydroxamic acids: Formation, structures, and reactivities. *Inorg. Chem.* **44**, 2934–2943.

Ghiorse, W. C., and Chapnick, S. D. (1983). Metal-depositing bacteria and the distribution of manganese and iron in swamp waters. *Ecol. Bull.* **35**, 367–376.

Ghiorse, W. C., and Hirsch, P. (1979). Ultrastructural-study of iron and manganese deposition associated with extracellular polymers of pedomicrobium-like budding bacteria. *Arch. Microbiol.* **123**, 213–226.

Ghosh, U., Talley, J. W., and Luthy, R. G. (2001). Particle-scale investigation of PAH desorption kinetics and thermodynamics from sediment. *Environ. Sci. Technol.* **35**, 3468–3475.

Goodhue, L. D., Hamilton, S., and Southam, G. (2005). The geomicrobiology of surficial geochemical anomalies. *Geochim. Cosmochim. Acta* **69**, A367.

Gordon, G. E., and Sturchio, N. C. (2002). An overview of synchrotron radiation applications to low temperature geochemistry and environmental science. *In* "Reviews in Mineralogy & Geochemistry" (P. A. Fenter, M. L. Rivers, N. C. Sturchio, and S. R. Sutton, Eds.), The Mineralogical Society of America, Vol. 69, pp. 1–116, Washington DC.

Gore, R. C. (1949). Infrared spectrometry of small samples with the reflecting microscope. *Science* **110**, 710–711.

Griffith, W. P., Lewis, J., and Wilkinson, G. (1959). Infrared spectra of transition metal-nitric oxide complexes.4. The pentacyanonitrosyl-complexes of chromium and molybdenum. *J. Am. Chem. Soc.* (MAR) 872–875.

Guilhaumou, N., Dumas, P., Carr, G. L., and Williams, G. P. (1998). Synchrotron infrared microspectrometry applied to petrography in micrometer-scale range: Fluid chemical analysis and mapping. *Appl. Spectrosc.* **52**(8), 1029–1034.

Ha, Y. W., Stack, R. J., Hespell, R. B., Gordon, S. H., and Bothast, R. J. (1991). Some chemical and physical-properties of extracellular polysaccharides produced by butyrivibrio-fibrisolvens strains. *Appl. Environ. Microbiol.* **57**, 2016–2020.

Hale, D. D., Rogers, J. E., and Wiegel, J. (1990a). Reductive dechlorination of dichlorophenols by nonadapted and adapted microbial communities in pond sediments. *Microbial Ecol.* **20**, 185–196.

Hale, D. D., Rogers, J. E., and Wiegel, J. W. (1990b). Reductive dechlorination of dichlorophenols in anaerobic pond sediments. *Abst. Pap. Am. Chem. S.* **199**, 137.

Haugland, R. P. (2002). "Handbook of Fluorescent Probes and Research Products," Molecular Probes. http://probes.invitrogen.com/

Hawkins, N. J., Mattraw, H. C., Sabol, W. W., and Carpenter, D. R. (1955). Spectroscopy of gaseous carbonyls.1. Infrared spectra and thermodynamic properties of chromium and molybdenum hexacarbonyls. *J. Chem. Phys.* **23**, 2422–2427.

Helm, D., and Naumann, D. (1995). Identification of some bacterial-cell components by FT-IR spectroscopy. *FEMS Microbiol. Lett.* **126**, 75–79.

Helm, D., Labischinski, H., and Naumann, D. (1991a). Elaboration of a procedure for identification of bacteria using Fourier-transform IR spectral libraries—a stepwise correlation approach. *J. Microbiol. Meth.* **14**, 127–142.

Helm, D., Labischinski, H., Schallehn, G., and Naumann, D. (1991b). Classification and identification of bacteria by Fourier-transform infrared-spectroscopy. *J. Gen. Microbiol.* **137**, 69–79.

Hines, M. E., Orem, W. H., Lyons, W. B., and Jones, G. E. (1982). Microbial activity and bioturbation induced oscillations in pore water chemistry of estuarine sediments in spring. *Nature* **299**, 433–435.

Hirschmugl, C. J. (2002a). Applications of storage ring infrared spectromicroscopy and reflection-absorption spectroscopy to geochemistry and environmental science. *Rev. Mineral. Geochem.* **49**, 317–339.

Hirschmugl, C. J. (2002b). Frontiers in infrared spectroscopy at surfaces and interfaces. *Surf. Sci.* **500**, 577–604.

Holman, H. N., Martin, M. C., Blakely, E. A., Bjornstad, K., and McKinney, W. R. (2000a). IR spectroscopic characteristics of cell cycle and cell death probed by synchrotron radiation based fourier transform IR spectromicroscopy. *Biopolymers* **57**, 329–335.

Holman, H. Y. N. (2004). Tracking microbial interactions with oxyanions by synchrotron infrared spectromicroscopy. *Abst. Pap. Am. Chem. S.* **228**, U619.

Holman, H. Y. N., Perry, D. L., and Hunter-Cevera, J. C. (1998). Surface-enhanced infrared absorption-reflectance (SEIRA) microspectroscopy for bacteria localization on geologic material surfaces. *J. Microbiol. Meth.* **34**, 59–71.

Holman, H. Y. N., Perry, D. L., Martin, M. C., Lamble, G. M., McKinney, W. R., and Hunter-Cevera, J. C. (1999). Real-time characterization of biogeochemical reduction of Cr(VI) on basalt surfaces by SR-FTIR imaging. *Geomicrobiol. J.* **16**, 307–324.

Holman, H. Y. N., Goth-Goldstein, R., Martin, M. C., Russell, M. L., and McKinney, W. R. (2000b). Low-dose responses to 2,3,7,8-tetrachlorodibenzo-p-dioxin in single living human cells measured by synchrotron infrared spectromicroscopy. *Environ. Sci. Technol.* **34**, 2513–2517.

Holman, H. Y. N., Bjornstad, K. A., McNamara, M. P., Martin, M. C., McKinney, W. R., and Blakely, E. A. (2002a). Synchrotron infrared spectromicroscopy as a novel bioanalytical microprobe for individual living cells: Cytotoxicity considerations. *J. Biomed. Opt.* **7**, 417–424.

Holman, H. Y. N., Nieman, K., Sorensen, D. L., Miller, C. D., Martin, M. C., Borch, T., McKinney, W. R., and Sims, R. C. (2002b). Catalysis of PAH biodegradation by humic acid shown in synchrotron infrared studies. *Environ. Sci. Technol.* **36**, 1276–1280.

Holman, H. Y. N., Martin, M. C., and McKinney, W. R. (2003). Tracking chemical changes in a live cell: Biomedical applications of SR-FTIR spectromicroscopy. *Spectrosc.—Int. J.* **17**, 139–159.

Holman, H. Y. N., Lin, Z., Asatiani, N. V., Kalabegishvili, T., Sapojnikova, N. A., Martin, M. C., McKinney, W. R., and Tsibakhashvili, N. Y. (2004). Role of the survival strategy of arthrobacters in the geochemical cycling of chromium—a spectroscopy and microscopy study. *Abst. Pap. Am. Chem. S.* **227**, U1221.

Hudgins, D. M., and Sandford, S. A. (1998a). Infrared spectroscopy of matrix isolated polycyclic aromatic hydrocarbons. 1. PAHs containing two to four rings. *J. Phys. Chem. A* **102**, 329–343.

Hudgins, D. M., and Sandford, S. A. (1998b). Infrared spectroscopy of matrix isolated polycyclic aromatic hydrocarbons. 2. PAHs containing five or more rings. *J. Phys. Chem. A* **102**, 344–352.

Hudgins, D. M., and Sandford, S. A. (1998c). Infrared spectroscopy of matrix isolated polycyclic aromatic hydrocarbons. 3. Fluoranthene and the benzofluoranthenes. *J. Phys. Chem. A* **102**, 353–360.

Hudgins, D. M., Bauschlicher, C. W., Allamandola, L. J., and Fetzer, J. C. (2000). Infrared spectroscopy of matrix-isolated polycyclic aromatic hydrocarbon ions. 5. PAHs incorporating a cyclopentadienyl ring. *J. Phys. Chem. A* **104**, 3655–3669.

Humphrey, R. E. (1961). The infrared spectra of aromatic chromium tricarbonyls. *Spectrochim. Acta* **17**, 93–100.

IARC (1990). "Monographs on the Evaluation of the Carcinogenic Risk of Chemicals to Humans." International Agency for Research on Cancer, Lyon, France.

Jamin, N., Dumas, P., Moncuit, J., Fridman, W. H., Teillaud, J. L., Carr, G. L., and Williams, G. P. (1998). Highly resolved chemical imaging of living cells by using synchrotron infrared microspectrometry. *Proc. Natl. Acad. Sci. USA* **95**, 4837–4840.

Janni, J., Gilbert, B. D., Field, R. W., and Steinfeld, J. I. (1997). Infrared absorption of explosive molecule vapors. *Spectrochim. Acta A* **53**, 1375–1381.

Jensen, J. O. (2004a). Vibrational frequencies and structural determination of arsenous tricyanide. *J. Mol. Struc.–Theochem.* **678**, 195–199.

Jensen, J. O. (2004b). Vibrational frequencies and structural determination of phosphorous tricyanide. *Spectrochim. Acta A* **60**, 2537–2540.

Jensen, J. O., and Jensen, J. L. (2004). Vibrational frequencies and structural determination of trimethylarsine oxide. *Spectrochim. Acta A* **60**, 3065–3070.

Joeckel, R. M., and Clement, B. J. A. (2005). Soils, surficial geology, and geomicrobiology of saline-sodic wetlands, North Platte River Valley, Nebraska, USA. *Catena* **61**, 63–101.

Jones, R. A., Koval, S. F., and Nesbitt, H. W. (2003). Surface alteration of arsenopyrite (FeAsS) by *Thiobacillus ferrooxidans*. *Geochim. Cosmochim. Acta* **67**, 955–965.

Jurgensen, A., Widmeyer, J. R., Gordon, R. A., Bendell-Young, L. I., Moore, M. M., and Crozier, E. D. (2004). The structure of the manganese oxide on the sheath of the bacterium *Leptothrix discophora:* An XAFS study. *Am. Mineral.* **89**, 1110–1118.

Kahng, L. S., and Shapiro, L. (2003). Polar localization of replicon origins in the multipartite genomes of *Agrobacterium tumefaciens* and *Sinorhizobium meliloti*. *J. Bacteriol.* **185**, 3384–3391.

Kalabegishvili, T. L., Tsibakhashvili, N. Y., and Holman, H. Y. N. (2003). Electron spin resonance study of chromium(V) formation and decomposition by basalt-inhabiting bacteria. *Environ. Sci. Technol.* **37**, 4678–4684.

Kalinowski, B. E., Liermann, L. J., Brantley, S. L., Barnes, A., and Pantano, C. G. (2000). X-ray photoelectron evidence for bacteria-enhanced dissolution of hornblende. *Geochim. Cosmochim. Acta* **64**, 1331–1343.

Kansiz, M., Heraud, P., Wood, B., Burden, F., Beardall, J., and McNaughton, D. (1999). Fourier transform infrared microspectroscopy and chemometrics as a tool for the discrimination of cyanobacterial strains. *Phytochemistry* **52**, 407–417.

Keller, W. D., Spotts, J. H., and Biggs, D. L. (1952). Infrared spectra of some rock-forming minerals. *Am. J. Sci.* **250**, 453.

Khijniak, T. V., Slobodkin, A. I., Coker, V., Renshaw, J. C., Livens, F. R., Bonch-Osmolovskaya, E. A., Birkeland, N. K., Medvedeva-Lyalikova, N. N., and Lloyd, J. R. (2005). Reduction of uranium(VI) phosphate during growth of the thermophilic bacterium *Thermoterrabacterium ferrireducens*. *Appl. Environ. Microbiol.* **71**, 6423–6426.

Kilkenny, D. M., Rocheleau, J. V., Piston, D. W., and Miller, G. G. (2002). c-Src expression decreases sensitivity to fibroblast growth factor (FGF)-1-induced chemotaxis and chemokinesis. *Mol. Biol. Cell* **13**, 329a.

Kim, Y. H., Pak, K., Pothuluri, J. V., and Cerniglia, C. E. (2004). Mineralization of erythromycin A in aquaculture sediments. *FEMS Microbiol. Lett.* **234**, 169–175.

Kirschner, C., Maquelin, K., Pina, P., Thi, N. A. N., Choo-Smith, L. P., Sockalingum, G. D., Sandt, C., Ami, D., Orsini, F., Doglia, S. M., Allouch, P., Mainfait, M., *et al.* (2001). Classification and identification of enterococci: A comparative phenotypic, genotypic, and vibrational spectroscopic study. *J. Clin. Microbiol.* **39**, 1763–1770.

Koenigsberg, S. S., Hazen, T. C., and Peacock, A. D. (2005). Environmental biotechnology: A bioremediation perspective. *Remediation Journal* **15,** 5–25.

Kretzschmar, R., Robarge, W. P., and Weed, S. B. (1993). Flocculation of kaolinitic soil clays: Effects of humic substances and iron-oxides. *Soil Sci. Soc. Am. J.* **57**, 1277–1283.

Krumholz, L. R., McKinley, J. P., Ulrich, F. A., and Suflita, J. M. (1997). Confined subsurface microbial communities in Cretaceous rock. *Nature* **386**, 64–66.

Kumamaru, T., Suenaga, H., Mitsuoka, M., Watanabe, T., and Furukawa, K. (1998). Enhanced degradation of polychlorinated biphenyls by directed evolution of biphenyl dioxygenase. *Nat. Biotechnol.* **16**, 663–666.

Labischinski, H., Naumann, D., Schultz, C., Kusumoto, S., Shiba, T., Rietschel, E. T., and Giesbrecht, P. (1989). Comparative X-Ray and Fourier-transform-infrared investigations of conformational properties of bacterial and synthetic lipid-a of *Escherichia coli* and *Salmonella minnesota* as well as partial structures and analogs thereof. *Eur. J. Biochem.* **179**, 659–665.

Lack, J. G., Chaudhuri, S. K., Kelly, S. D., Kemner, K. M., O'Connor, S. M., and Coates, J. D. (2002). Immobilization of radionuclides and heavy metals through anaerobic bio-oxidation of Fe(II). *Appl. Environ. Microbiol.* **68**, 2704–2710.

Lajtha, K., and Schlesinger, W. H. (1988). The biogeochemistry of phosphorus cycling and phosphorus availability along a desert soil chronosequence. *Ecology* **69**, 24–39.

Lang, P. L., and Sang, S. C. (1998). The *in situ* infrared microspectroscopy of bacterial colonies on agar plates. *Cell. Mol. Biol.* **44**, 231–238.

Latouche, G., Cerovic, Z. G., Montagnini, F., and Moya, I. (2000). Light-induced changes of NADPH fluorescence in isolated chloroplasts: A spectral and fluorescence lifetime study. *BBA–Bioenergetics* **1460**, 311–329.

Leveille, R. J., Fyfe, W. S., and Longstaffe, F. J. (2000). Geomicrobiology of carbonate-silicate microbialites from Hawaiian basaltic sea caves. *Chem. Geol.* **169**, 339–355.

Levina, A., Barr-David, G., Codd, R., Lay, P. A., Dixon, N. E., Hammershoi, A., and Hendry, P. (1999). *In vitro* plasmid DNA cleavage by chromium(V) and -(IV) 2-hydroxycarboxylato complexes. *Chem. Res. Toxicol.* **12**, 371–381.

Levina, A., Codd, R., Dillon, C. T., and Lay, P. A. (2003). Chromium in biology: Toxicology and nutritional aspects. *Prog. Inorg. Chem.* **51**, 145–250.

Levina, A., Codd, R., Foran, G. J., Hambley, T. W., Maschmeyer, T., Masters, A. F., and Lay, P. A. (2004). X-ray absorption spectroscopic studies of chromium(V/IV/III)2-ethyl-2-hydroxybutanoato(2-/1-) complexes. *Inorg. Chem.* **43**, 1046–1055.

Levinson, E., Lerch, P., and Martin, M. C. (2006). Infrared imaging: Synchrotrons vs. arrays, resolution vs. speed. *Infrared Phys. Techn.* (in press).

Li, J. F., Fuller, S., Cattle, J., Way, C. P., and Hibbert, D. B. (2004). Matching fluorescence spectra of oil spills with spectra from suspect sources. *Anal. Chim. Acta* **514**, 51–56.

Li, Z. R., Shokes, J. E., Kounosu, A., Imai, T., Iwasaki, T., and Scott, R. A. (2003). X-ray absorption spectroscopic analysis of reductive [2Fe-2S] cluster degradation in hyperthermophilic archaeal succinate: Caldariellaquinone oxidoreductase subunits. *Biochemistry* **42**, 15003–15008.

Lieberman, R. L., Shrestha, D. B., Doan, P. E., Hoffman, B. M., Stemmler, T. L., and Rosenzweig, A. C. (2003). Purified particulate methane monooxygenase from *Methylococcus capsulatus* (Bath) is a dimer with both mononuclear copper and a copper-containing cluster. *Proc. Natl. Acad. Sci. USA* **100**, 3820–3825.

Lijour, Y., Gentric, E., Deslandes, E., and Guezennec, J. (1994). Estimation of the sulfate content of hydrothermal vent bacterial polysaccharides by Fourier-transform infrared-spectroscopy. *Anal. Biochem.* **220**, 244–248.

Lovley, D. R., and Phillips, E. J. P. (1992). Reduction of uranium by *Desulfovibrio desulfuricans*. *Appl. Environ. Microbiol.* **58**, 850–856.

Lovley, D. R., and Woodward, J. C. (1996). Mechanisms for chelator stimulation of microbial Fe(III)-oxide reduction. *Chem. Geol.* **132**, 19–24.

Lovley, D. R., Roden, E. E., Phillips, E. J. P., and Woodward, J. C. (1993a). Enzymatic iron and uranium reduction by sulfate-reducing bacteria. *Mar. Geol.* **113**, 41–53.

Lovley, D. R., Widman, P. K., Woodward, J. C., and Phillips, E. J. P. (1993b). Reduction of uranium by cytochrome-C(3) of *Desulfovibrio vulgaris*. *Appl. Environ. Microbiol.* **59**, 3572–3576.

Lu, R., Goncharov, A., Mao, H. K., and Hemley, R. (1999). Synchrotron infrared microspectroscopy: Applications to hydrous minerals. *In* "Synchrotron X-ray Methods in Clay Sciences" (D. G. Schulze, J. W. Stucki, and P. M. Bertsch, Eds.), pp. 164–182. The Clay Mineral Society, Boulder.

Ludwig, C., Dolny, M., and Gotze, H. J. (2000). Fourier transform Raman and infrared spectra and normal coordinate analysis of organo-arsenic(III), -antimony(III) and -bismuth(III) thiolates. *Spectrochim. Acta A* **56**, 547–555.

Luys, M. J., Deroy, G., Vansant, E. F., and Adams, F. (1982). Characteristics of asbestos minerals: Structural aspects and infrared-spectra. *J. Chem. Soc.–Faraday T. I* **78**, 3561–3571.

Lyons, W. B., Gaudette, H. E., and Armstrong, P. B. (1979). Evidence for organically associated iron in nearshore pore fluids. *Nature* **282**, 202–203.

Macalady, J., and Banfield, J. F. (2003). Molecular geomicrobiology: Genes and geochemical cycling. *Earth Planet. Sc. Lett.* **209**, 1–17.

Maquelin, K., Kirschner, C., Choo-Smith, L. P., van den Braak, N., Endtz, H. P., Naumann, D., and Puppels, G. J. (2002). Identification of medically relevant microorganisms by vibrational spectroscopy (Review). *J. Microbiol. Meth.* **51**, 255–271.

Maquelin, K., Kirschner, C., Choo-Smith, L. P., Ngo-Thi, N. A., van Vreeswijk, T., Stammler, M., Endtz, H. P., Bruining, H. A., Naumann, D., and Puppels, G. J. (2003). Prospective study of the performance of vibrational spectroscopies for rapid identification of bacterial and fungal pathogens recovered from blood cultures. *J. Clin. Microbiol.* **41**, 324–329.

Martin, M. C., Tsvetkova, N. M., Crowe, J. H., and McKinney, W. R. (2001). Negligible sample heating from synchrotron infrared beam. *Appl. Spectrosc.* **55**, 111–113.

Mattioda, A. L., Hudgins, D. M., Bauschlicher, C., and Allamandola, L. J. (2002). Infrared spectra of matrix-isolated polycyclic aromatic hydrocarbons and their ions: PAHs incorporating the peropyrene structure. *Abst. Pap. Am. Chem. S.* **224**, U323.

Maurice, P. A., Vierkorn, M. A., Hersman, L. E., and Fulghum, J. E. (2001). Dissolution of well and poorly ordered kaolinites by an aerobic bacterium. *Chem. Geol.* **180**, 81–97.

McCann, M. C., Hammouri, M., Wilson, R., Belton, P., and Roberts, K. (1992). Fourier-transform infrared microspectroscopy is a new way to look at plant-cell walls. *Plant Physiol.* **100**, 1940–1947.

McKinney, W. R., Martin, M. C., Chin, M., Portman, G., Melczer, M. E., and Watson, J. A. (2000). 4 Axis implementation of the active feedback mirror system for the IR beamline 1.4.3. *ALS Compendium.* http://infrared.als.lbl.gov/

McMahon, P. B., and Chapelle, F. H. (1991). Microbial-production of organic-acids in aquitard sediments and its role in aquifer geochemistry. *Nature* **349**, 233–235.

Merroun, M. L., Raff, J., Rossberg, A., Hennig, C., Reich, T., and Selenska-Pobell, S. (2005). Complexation of uranium by cells and S-layer sheets of *Bacillus sphaericus* JG-A12. *Appl. Environ. Microbiol.* **71**, 5532–5543.

Mielczarski, J. A., Cases, J. M., Bouquet, E., Barres, O., and Delon, J. F. (1993). Nature and structure of adsorption layer on apatite contacted with oleate solution.1. Adsorption and Fourier-transform infrared reflection studies. *Langmuir* **9**, 2370–2382.

Miller, D. N., Yavitt, J. B., Madsen, E. L., and Ghiorse, W. C. (2004). Methanotrophic activity, abundance, and diversity in forested swamp pools: Spatiotemporal dynamics and influences on methane fluxes. *Geomicrobiol. J.* **21**, 257–271.

Miller, L. M., Carlson, C. S., Carr, G. L., and Chance, M. R. (1998). A method for examining the chemical basis for bone disease: Synchrotron infrared microspectroscopy. *Cell. Mol. Biol.* **44**, 117–127.

Miller, L. M., Dumas, P., Jamin, N., Teillaud, J. L., Bantignies, J. L., and Carr, G. L. (2000). Applications of synchrotron infrared microspectroscopy to the study of biological cells and tissues. *Inst. Phys. Conf. Ser.* **165**, 75–76.

Miller, L. M., Dumas, P., Jamin, N., Teillaud, J. L., Miklossy, J., and Forro, L. (2002). Combining IR spectroscopy with fluorescence imaging in a single microscope: Biomedical applications using a synchrotron infrared source (invited). *Rev. Sci. Instrum.* **73**, 1357–1360.

Misawa, N., Shindo, K., Takahashi, H., Suenaga, H., Iguchi, K., Okazaki, H., Harayama, S., and Furukawa, K. (2002). Hydroxylation of various molecules including heterocyclic aromatics using recombinant *Escherichia coli* cells expressing modified biphenyl dioxygenase genes. *Tetrahedron* **58**, 9605–9612.

Naumann, D., Barnickel, G., Bradaczek, H., Labischinski, H., and Giesbrecht, P. (1982). Infrared-spectroscopy, a tool for probing bacterial peptidoglycan: Potentialities of infrared-spectroscopy for cell-wall analytical studies and rejection of models based on crystalline chitin. *Eur. J. Biochem.* **125**, 505–515.

Naumann, D., Fijala, V., Labischinski, H., and Giesbrecht, P. (1988). The rapid differentiation and identification of pathogenic bacteria using Fourier-transform infrared spectroscopic and multivariate statistical-analysis. *J. Mol. Struct.* **174**, 165–170.

Naumann, D., Schultz, C. P., and Helm, D. (1996). What can infrared spectroscopy tell us about the structure and composition of intact bacterial cells? *In* "Infrared Spectroscopy of Biomolecules" (H. H. Mantsch and D. Chapman, Eds.), pp. 279–310. Wiley-Liss, New York.

Neal, A. L., Amonette, J. E., Peyton, B. M., and Geesey, G. G. (2004a). Uranium complexes formed at hematite surfaces colonized by sulfate-reducing bacteria. *Environ. Sci. Technol.* **38**, 3019–3027.

Neal, A. L., Clough, L. K., Perkins, T. D., Little, B. J., and Magnuson, T. S. (2004b). *In situ* measurement of Fe(III) reduction activity of Geobacter pelophilus by simultaneous *in situ* RT-PCR and XPS analysis. *FEMS Microbiol. Ecol.* **49**, 163–169.

Nesterova, M., Moreau, J., and Banfield, J. F. (2003). Model biomimetic studies of templated growth and assembly of nanocrystalline FeOOH. *Geochim. Cosmochim. Acta* **67**, 1177–1187.

Newo, A. N. S., Pshenichnikova, A. B., Skladnev, D. A., and Shvets, V. I. (2004). Deuterium oxide as a stress factor for the methylotrophic bacterium Methylophilus sp. B-7741. *Microbiology* **73**, 139–142.

Ngo-Thi, N. A., Kirschner, C., and Naumann, D. (2003). Characterization and identification of microorganisms by FIF-IR microspectrometry. *J. Mol. Struct.* **661**, 371–380.

Nguyen, T. T., Janik, L. J., and Raupach, M. (1991). Diffuse reflectance infrared Fourier-transform (drift) spectroscopy in soil studies. *Aust. J. Soil Res.* **29**, 49–67.

Orser, C. S., Foong, F. C. F., Capaldi, R., Nalezny, J., Mackay, W., Benjamin, M., and Farr, S. B. (1995). Use of prokaryotic stress promoters as indicators of the mechanisms of chemical toxicity. *In vitro Toxicol.* **8**, 71–85.

Osborne, F. H., and Ehrlich, H. L. (1976). Oxidation of arsenite by a soil isolate of Alcaligenes. *J. Appl. Bacteriol.* **41**, 295–305.

Panak, P. J., Knopp, R., Booth, C. H., and Nitsche, H. (2002). Spectroscopic studies on the interaction of U(VI) with Bacillus sphaericus. *Radiochim. Acta* **90**, 779–783.

Panero, W. R., Benedetti, L. R., and Jeanloz, R. (2003). Transport of water into the lower mantle: Role of stishovite. *J. Geophys. Res.-Sol. Ea.* **108**(B1), 2039–2047.

Pauzat, F., and Ellinger, Y. (2001). The 3.2–3.5 mu m region revisited–II. A theoretical study of the effects of hydrogenation on some model PAHs. *Mon. Not. R. Astron. Soc.* **324**, 355–366.

Pauzat, F., and Ellinger, Y. (2002). The infrared signatures of non-regular PAHs. *Chem. Phys.* **280**, 267–282.

Peitscher, G. W. (1986). Infrared microspectroscopy of polymers. *Makromol. Chem.-M. Symp.* **5**, 75–85.

Pennisi, E. (2000). Geomicrobiology: Hardy microbe thrives at pH 0. *Science* **287**, 1731–1732.

Phillips, E. J. P., Landa, E. R., and Lovley, D. R. (1995). Remediation of uranium contaminated soils with bicarbonate extraction and microbial U(VI) reduction. *J. Ind. Microbiol.* **14**, 203–207.

Pickering, I. J., George, G. N., Yu, E. Y., Brune, D. C., Tuschak, C., Overmann, J., Beatty, J. T., and Prince, R. C. (2001). Analysis of sulfur biochemistry of sulfur bacteria using X-ray absorption spectroscopy. *Biochemistry* **40**, 8138–8145.

Piston, D. W., and Knobel, S. M. (1999). Real-time analysis of glucose metabolism by microscopy. *Trends Endocrin. Met.* **10**, 413–417.

Plesko, E. P., Scheetz, B. E., and White, W. B. (1992). Infrared vibrational characterization and synthesis of a family of hydrous alkali uranyl silicates and hydrous uranyl silicate minerals. *Am. Mineral.* **77**, 431–437.

Pothuluri, J. V., Selby, A., Evans, F. E., Freeman, J. P., and Cerniglia, C. E. (1995). Transformation of chrysene and other polycyclic aromatic hydrocarbon mixtures by the fungus *Cunninghamella-elegans*. *Can. J. Bot.-Revue Canadienne De Botanique* **73**, S1025–S1033.

Pothuluri, J. V., Doerge, D. R., Churchwell, M. I., Fu, P. P., and Cerniglia, C. E. (1998a). Fungal metabolism of nitrofluoranthenes. *J. Toxicol. Environ. Health-Part A* **53**, 153–174.

Pothuluri, J. V., Sutherland, J. B., Freeman, J. P., and Cerniglia, C. E. (1998b). Fungal biotransformation of 6-nitrochrysene. *App. Environ. Microbiol.* **64**, 3106–3109.

Pothuluri, J. V., Freeman, J. P., Fu, P. P., and Cerniglia, C. E. (1999). Biotransformation of 1-nitrobenzo[e]pyrene by the fungus *Cunninghamella elegans*. *J. Indust. Microbiol. Biotechn.* **22**, 52–57.

Povarennykh, A. S. (1978). Use of infrared-spectra for determination of minerals. *Am. Mineral.* **63**, 956–959.

Prange, A., Chauvistre, R., Modrow, H., Hormes, J., Truper, H. G., and Dahl, C. (2002a). Quantitative speciation of sulfur in bacterial sulfur globules: X-ray absorption spectroscopy reveals at least three different species of sulfur. *Microbiol.-Sgm* **148**, 267–276.

Prange, A., Dahl, C., Truper, H. G., Behnke, M., Hahn, J., Modrow, H., and Hormes, J. (2002b). Investigation of S-H bonds in biologically important compounds by sulfur K-edge X-ray absorption spectroscopy. *Eur. Phys. J. D* **20**, 589–596.

Pshenichnikova, A. B., Nevo, A. N. S., Volkova, E. V., Skladnev, D. A., and Shvets, V. I. (2004). Effect of deuteration on the activity of methanol dehydrogenase from Methylophilus sp B-7741. *Appl. Biochem. Microbiol.* **40**, 18–21.

Raab, T. K., and Vogel, J. P. (2004). Ecological and agricultural applications of synchrotron IR microscopy. *Infrared Phys. Techn.* **45**, 393–402.

Reffner, J. A., Martoglio, P. A., and Williams, G. P. (1995). Fourier-transform infrared microscopic analysis with synchrotron-radiation: The microscope optics and system performance. *Rev. Sci. Instrum.* **66**, 1298–1302.

Reffner, J. A., Carr, G. L., and Williams, G. P. (1997). Infrared microspectroscopy with synchrotron radiation. *Mikrochim. Acta* (Suppl. 14), 339–341.

Renault, P., Calero, S., Delorme, C., Drouault, S., Goupil-Feuillerat, N., Guedon, E., and Ehrlich, S. D. (1998). From genome to industrial application. *Lait* **78**, 39–52.

Renshaw, J. C., Butchins, L. J. C., Livens, F. R., May, I., Charnock, J. M., and Lloyd, J. R. (2005). Bioreduction of uranium: Environmental implications of a pentavalent intermediate. *Environ. Sci. Techn.* **39**, 5657–5660.

Revsbech, N. P., Sorensen, J., Blackburn, T. H., and Lomholt, J. P. (1980). Distribution of oxygen in marine-sediments measured with microelectrodes. *Limnol. Oceanogr.* **25**, 403–411.

Rocheleau, J. V., Edidin, M., and Piston, D. W. (2002). Monitoring the membrane rotational mobility of MHC class I protein using an intra-sequence expressed GFP construct. *Biophys. J.* **82**, 627a.

Rogers, J. E., and Hale, D. D. (1987). Anaerobic degradation of dichlorophenol isomers in fresh-water pond sediments. *Abst. Pap. Am. Chem. S.* **194**, 244.

Rossman, G. R., and Aines, R. D. (1991). The hydrous components in garnets—grossular-hydrogrossular. *Am. Mineral.* **76**, 1153–1164.

Ruiterkamp, R., Halasinski, T., Salama, F., Foing, B. H., Allamandola, L. J., Schmidt, W., and Ehrenfreund, P. (2002). Spectroscopy of large PAHs: Laboratory studies and comparison to the diffuse interstellar bands. *Astron. Astrophys.* **390**, 1153–1170.

Saita, S., and Maenosono, S. (2005). FePt nanoparticles with a narrow composition distribution synthesized via pyrolysis of iron(III) ethoxide and platinum(II) acetylacetonate. *Chem. Mater.* **17**, 3705–3710.

Salisbury, J. W., Walter, L. S., Vergo, N., and D'Aria, D. M. (1991). "Infrared (2.1–25 μm) Spectra of Minerals." The Johns Hopkins University Press, Baltimore and London.

Sanchez-Moral, S., Canaveras, J. C., Laiz, L., Saiz-Jimenez, C., Bedoya, J., and Luque, L. (2003). Biomediated precipitation of calcium carbonate metastable phases in hypogean environments: A short review. *Geomicrobiol. J.* **20**, 491–500.

Sarret, G., Avoscan, L., Carriere, M., Collins, R., Geoffroy, N., Carrot, F., Coves, J., and Gouget, B. (2005). Chemical forms of selenium in the metal-resistant bacterium *Ralstonia metallidurans* CH34 exposed to selenite and selenate. *Appl. Environ. Microbiol.* **71**, 2331–2337.

Scarvie, T., Andresen, N., Baptiste, K., Byrd, J., Chin, M., Martin, M. C., McKinney, W. R., and Steier, C. (2004). Noise reduction efforts for the ALS infrared beamlines. *Infrared Phys. Techn.* **45**, 403–408.

Schabereiter-Gurtner, C., Saiz-Jimenez, C., Pinar, G., Lubitz, W., and Rolleke, S. (2002). Phylogenetic 16S rRNA analysis reveals the presence of complex and partly unknown bacterial communities in Tito Bustillo cave, Spain, and on its Palaeolithic paintings. *Environ. Microbiol.* **4**, 392–400.

Schultz, C., and Naumann, D. (1991). *In vivo* study of the state of order of the membranes of gram-negative bacteria by Fourier-transform infrared-spectroscopy (Ft-Ir). *FEBS Lett.* **294**, 43–46.

Schultz, C., Labischinski, H., and Naumann, D. (1987). Thermotropic phase-behavior of gram-negative bacterial lipopolysaccharides studied using Fourier-transform infrared-spectroscopy (Ft-Ir). *Z. Kristallogr.* **178**, 201–202.

Seelenbinder, J. A., and Brown, C. W. (2002). Comparison of organic self-assembled monolayers as modified substrates for surface-enhanced infrared absorption spectroscopy. *Appl. Spectrosc.* **56**, 295–299.

Sham, T. K., and Rivers, M. L. (2002). A brief overview of synchrotron radiation. *Rev. Mineral Geochem.* **49**, 117–147.

Simon, D., Muller, R. H., Bley, T., and Babel, W. (1996). Correlation between cellular fluorescence and NAD(P)H levels in Alcaligenes eutrophus JMP 134. *Bioprocess Eng.* **14**, 57–62.

Sinclair, J. L., and Ghiorse, W. C. (1989). Distribution of aerobic-bacteria, protozoa, algae, and fungi in deep subsurface sediments. *Geomicrobiol. J.* **7**, 15–31.

Snow, E. T. (1991). A possible role for chromium(III) in genotoxicity. *Environ. Health Persp.* **92**, 75–81.

Sorensen, J., Jorgensen, B. B., and Revsbech, N. P. (1979). Comparison of oxygen, nitrate, and sulfate respiration in coastal marine-sediments. *Microb. Ecol.* **5**, 105–115.

Spilde, M. N., Northup, D. E., Boston, P. J., Schelble, R. T., Dano, K. E., Crossey, L. J., and Dahm, C. N. (2005). Geomicrobiology of cave ferromanganese deposits: A field and laboratory investigation. *Geomicrobiol. J.* **22**, 99–116.

Sreedhara, A., Susa, N., and Rao, C. P. (1997). Vanadate and chromate reduction by saccharides and L-ascorbic acid: Effect of the isolated V(IV) and Cr(III) products on DNA nicking, lipid peroxidation, cytotoxicity and on enzymatic and non-enzymatic antioxidants. *Inorg. Chim. Acta* **263**, 189–194.

Stern, R. M. (1982). Biological and environmental aspects of chromium. *In* "Biological and Environmental Aspects of Chromium" (S. Langard, Ed.). Elsevier, Amsterdam.

Suenaga, H., Mitsuoka, M., Ura, Y., Watanabe, T., and Furukawa, K. (2001). Directed evolution of biphenyl dioxygenase: Emergence of enhanced degradation capacity for benzene, toluene, and alkylbenzenes. *J. Bacteriol.* **183**, 5441–5444.

Suenaga, H., Watanabe, T., Sato, M., Furukawa, N., and Furukawa, K. (2002). Alteration of regiospecificity in biphenyl dioxygenase by active-site engineering. *J. Bacteriol.* **184**, 3682–3688.

Suzuki, Y., and Banfield, J. F. (2004). Resistance to, and accumulation of, uranium by bacteria from a uranium-contaminated site. *Geomicrobiol. J.* **21**, 113–121.

Suzuki, Y., Kelly, S. D., Kemner, K. A., and Banfield, J. F. (2003). Microbial populations stimulated for hexavalent uranium reduction in uranium mine sediment. *Appl. Environ. Microbiol.* **69**, 1337–1346.

Tebo, B. M., Ghiorse, W. C., vanWaasbergen, L. G., Siering, P. L., and Caspi, R. (1997). Bacterially mediated mineral formation: Insights into manganese(II) oxidation from molecular genetic and biochemical studies. *Rev. Mineral* **35**, 225–266.

Tebo, B. M., Bargar, J. R., Clement, B. G., Dick, G. J., Murray, K. J., Parker, D., Verity, R., and Webb, S. M. (2004). Biogenic manganese oxides: Properties and mechanisms of formation. *Annu. Rev. Earth Pl. Sc.* **32**, 287–328.

Tebo, B. M., Johnson, H. A., McCarthy, J. K., and Templeton, A. S. (2005). Geomicrobiology of manganese(II) oxidation. *Trends Microbiol.* **13**, 421–428.

Templeton, A. S., Staudigel, H., and Tebo, B. M. (2005). Diverse Mn(II)-oxidizing bacteria isolated from submarine basalts at Loihi Seamount. *Geomicrobiol. J.* **22**, 127–139.

Thanbichler, M., Viollier, P. H., and Shapiro, L. (2005). The structure and function of the bacterial chromosome. *Curr. Opin. Gen. Dev.* **15**, 153–162.

Todd, M. W., Provencal, R. A., Owano, T. G., Paldus, B. A., Kachanov, A., Vodopyanov, K. L., Hunter, M., Coy, S. L., Steinfeld, J. I., and Arnold, J. T. (2002). Application of mid-infrared cavity-ringdown ectroscopy to trace explosives vapor detection using a broadly tunable (6–8 μm) optical parametric oscillator. *Appl. Phys. B-Lasers O.* **75**, 367–376.

Toner, B., Fakra, S., Villalobos, M., Warwick, T., and Sposito, G. (2005). Spatially resolved characterization of biogenic manganese oxide production within a bacterial biofilm. *Appl. Environ. Microbiol.* **71**, 1300–1310.

Tsibakhashvili, N. Y., Asatiani, N. V., Abuladze, M. K., Birkaya, B. G., Sapojnikova, N. A., Mosulishvili, L. M., and Holman, H. Y. N. (2002a). Capillary electrophoresis of Cr(VI) reducer *Arthrobacter oxydans*. *Biomed. Chromatogr.* **16**, 327–331.

Tsibakhashvili, N. Y., Mosulishvili, L. M., Kalabegishvili, T. L., Pataraya, D. T., Gurielidze, M. A., Nadareishvili, G. S., and Holman, H. Y. N. (2002b). Chromate-resistant and reducing-microorganisms in georgia basalts: Their distribution and characterization. *Fresen. Environ. Bull.* **11**, 352–361.

Tsibakhashvili, N. Y., Mosulishvili, L. M., Kalabegishvili, T. L., Kirkesali, E. I., Frontasyeva, M. V., Pomyakushina, E. V., Pavlov, S. S., and Holman, H. Y. N. (2004). ENAA studies of chromium uptake by *Arthrobacter oxydans*. *J. Radioanal. Nucl. Chem.* **259**, 527–531.

Tsou, T. C., Lin, R. J., and Yang, J. L. (1997). Mutational spectrum induced by chromium(III) in shuttle vectors replicated in human cells: Relationship to Cr(III)-DNA interactions. *Chem. Res. Toxicol.* **10**, 962–970.

Twining, B. S., Baines, S. B., Fisher, N. S., and Landry, M. R. (2004). Cellular iron contents of plankton during the southern ocean iron experiment (SOFeX). *Deep-Sea Res.* **51**, 1827–1850.

Vandermei, H. C., Naumann, D., and Busscher, H. J. (1993). Grouping of oral streptococcal species using Fourier-transform infrared-spectroscopy in comparison with classical microbiological identification. *Arch. Oral Biol.* **38**, 1013–1019.

Vandermei, H. C., Naumann, D., and Busscher, H. J. (1996). Grouping of *Streptococcus mitis* strains grown on different growth media by Ft-Ir. *Infrared Phys. Techn.* **37**, 561–564.

Vandyk, T. K., Smulski, D. R., Reed, T. R., Belkin, S., Vollmer, A. C., and Larossa, R. A. (1995). Responses to toxicants of an *Escherichia coli* strain carrying a Uspa'–Lux genetic fusion and an *Escherichia coli* strain carrying a Grpe'–Lux fusion are similar. *Appl. Environ. Microbiol.* **61**, 4124–4127.

Vilas, F., Jarvis, K. S., and Gaffey, M. J. (1994). Iron alteration minerals in the visible and near-infrared spectra of low-Albedo asteroids. *Icarus* **109**, 274–283.

Viollier, P. H., and Shapiro, L. (2004). Spatial complexity of mechanisms controlling a bacterial cell cycle. *Curr. Opin. Microbiol.* **7**, 572–578.

Viollier, P. H., Sternheim, N., and Shapiro, L. (2002). A dynamically localized histidine kinase controls the asymmetric distribution of polar pili proteins. *EMBO J.* **21**, 4420–4428.

Vogel, J. P., Raab, T. K., Schiff, C., and Somerville, S. C. (2002). PMR6, a pectate lyase-like gene required for powdery mildew susceptibility in *Arabidopsis*. *Plant Cell* **14**, 2095–2106.

Vogel, J. P., Raab, T. K., Somerville, C. R., and Somerville, S. C. (2004). Mutations in PMR5 result in powdery mildew resistance and altered cell wall composition. *Plant J.* **40**, 968–978.

Vogt, S., Maser, J., and Jacobsen, C. (2003). Data analysis for X-ray fluorescence imaging. *J. Phys. IV* **104**, 617–622.

Voitkun, V., Zhitkovich, A., and Costa, M. (1998). Cr(III)-mediated crosslinks of glutathione or amino acids to the DNA phosphate backbone are mutagenic in human cells. *Nucleic Acids Res.* **26**, 2024–2030.

Watson, J. H. P., and Ellwood, D. C. (2003). The removal of the pertechnetate ion and actinides from radioactive waste streams at Hanford, Washington, USA and Sellafield, Cumbria, UK: The role of iron-sulfide-containing adsorbent materials. *Nucl. Eng. Des.* **226**, 375–385.

Watson, J. H. P., Cressey, B. A., Roberts, A. P., Ellwood, D. C., Charnock, J. M., and Soper, A. K. (2000). Structural and magnetic studies on heavy-metal-adsorbing iron sulphide nanoparticles produced by sulphate-reducing bacteria. *J. Magn. Magn. Mater.* **214**, 13–30.

Weijer, C. J. (2003). Visualizing signals moving in cells. *Science* **300**, 96–100.

Welch, S. A., Taunton, A. E., and Banfield, J. F. (2002). Effect of microorganisms and microbial metabolites on apatite dissolution. *Geomicrobiol. J.* **19**, 343–367.

Wellsbury, P., Mather, I., and Parkes, R. J. (2002). Geomicrobiology of deep, low organic carbon sediments in the Woodlark Basin, Pacific Ocean. *FEMS Microbiol. Ecol.* **42**, 59–70.

Wetzel, D. L., Eilert, A. J., Pietrzak, L. N., Miller, S. S., and Sweat, J. A. (1998). Ultraspatially resolved synchrotron infrared microspectroscopy of plant tissue *in situ*. *Cell. Mol. Biol.* **44**, 145–168.

Wetzel, D. L., Post, G. R., and Lodder, R. A. (2005). Synchrotron infrared micro spectroscopic analysis of collagens I, III, and elastin on the shoulders of human thin-cap fibroatheromas. *Vibr. Spectrosc.* **38**, 53–59.

White, J. L. (1971). Interpretation of infrared spectra of soil minerals. *Soil Science* **112**, 22.

Wildung, R. E., Li, S. W., Murray, C. J., Krupka, K. M., Xie, Y., Hess, N. J., and Roden, E. E. (2004). Technetium reduction in sediments of a shallow aquifer exhibiting dissimilatory iron reduction potential. *FEMS Microbiol. Ecol.* **49**, 151–162.

Yee, N., and Benning, L. G. (2002). *In situ* FTIR study of protonation reactions at the bacteria-water interface. *Geochim. Cosmochim. Acta* **66**, A862.

Yee, N., Phoenix, V. R., Konhauser, K. O., Benning, L. G., and Ferris, F. G. (2003). The effect of cyanobacteria on silica precipitation at neutral pH: Implications for bacterial silicification in geothermal hot springs. *Chem. Geol.* **199**, 83–90.

Yee, N., Benning, L. G., and Konhauser, K. O. (2004a). Silica colloid aggregation by cyanobacteria: A microbial silicification mechanism. *Geochim. Cosmochim. Acta* **68**, A199.

Yee, N., Benning, L. G., Phoenix, V. R., and Ferris, F. G. (2004b). Characterization of metal-cyanobacteria sorption reactions: A combined macroscopic and infrared spectroscopic investigation. *Environ. Sci. Techn.* **38**, 775–782.

Yu, P. (2005a). Molecular chemistry imaging to reveal structural features of various plant feed tissues. *J. Struct. Biol.* **150**, 81–89.

Yu, P., Christensen, D. A., Christensen, C. R., Drew, M. D., Rossnagel, B. G., and McKinnon, J. J. (2004). Use of synchrotron FTIR microspectroscopy to identify chemical differences in barley endosperm tissue in relation to rumen degradation characteristics. *Can. J. Animal Sci.* **84**, 523–527.

Yu, P. Q. (2005b). Application of cluster analysis (CLA) in feed chemical imaging to accurately reveal structural-chemical features of feeds and plants within cellular dimension. *J. Agric. Food Chem.* **53**, 2872–2880.

Yu, P. Q., McKinnon, J. J., Christensen, C. R., Christensen, D. A., Marinkovic, N. S., and Miller, L. M. (2003). Chemical imaging of microstructures of plant tissues within cellular dimension using synchrotron infrared microspectroscopy. *J. Agric. Food Chem.* **51**, 6062–6067.

Zhang, C. L. L., and Lanoil, B. (2004). Geomicrobiology and biogeochemistry of gas hydrates and cold seeps. *Chem. Geol.* **205**, 187–194.

Zhang, Q. H., Piston, D. W., and Goodman, R. H. (2002). Regulation of corepressor function by nuclear NADH. *Science* **295**, 1895–1897.

Zhang, Y., Yang, M., Dou, X. M., He, H., and Wang, D. S. (2005). Arsenate adsorption on an Fe-Ce bimetal oxide adsorbent: Role of surface properties. *Environ. Sci. Techn.* **39**, 7246–7253.

Zouboulis, A. I., and Katsoyiannis, I. A. (2005). Recent advances in the bioremediation of arsenic-contaminated groundwaters. *Environ. Int.* **31**, 213–219.

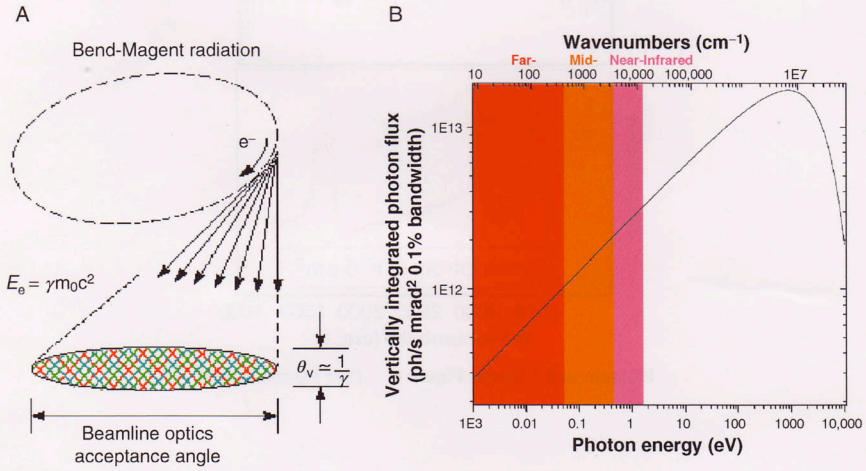

Holman and Martin, Figure 3 (See legend in text.)

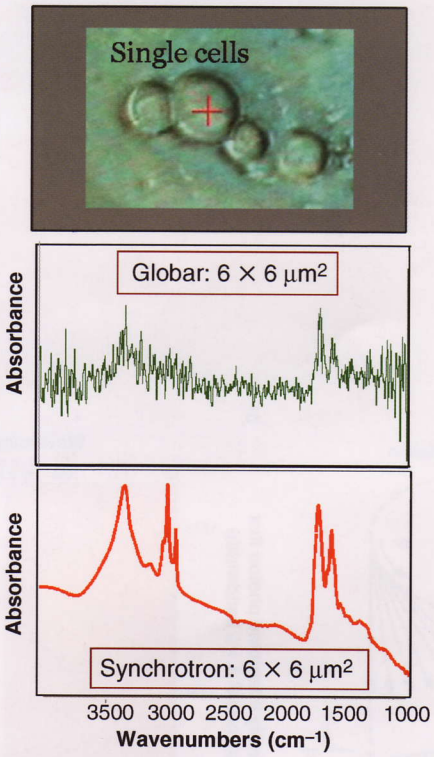

Holman and Martin, Figure 6 (See legend in text.)

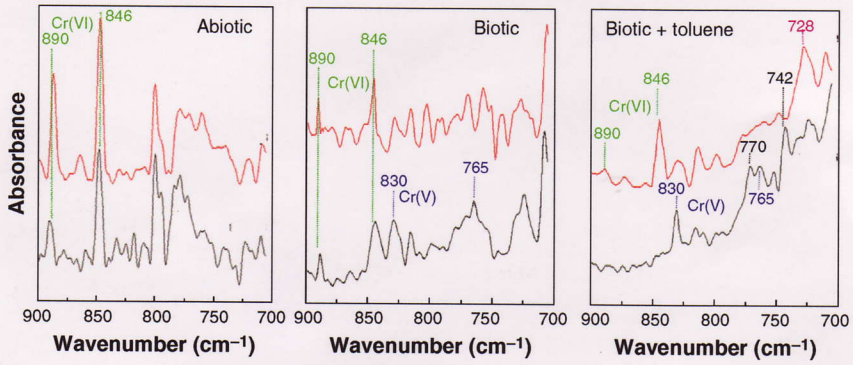

Holman and Martin, Figure 8 (See legend in text.)

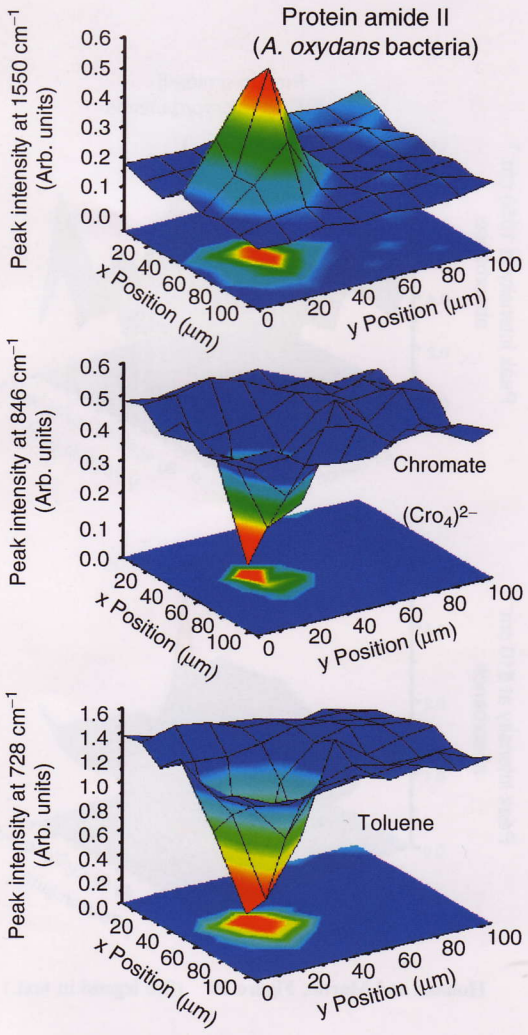

Holman and Martin, Figure 9 (See legend in text.)

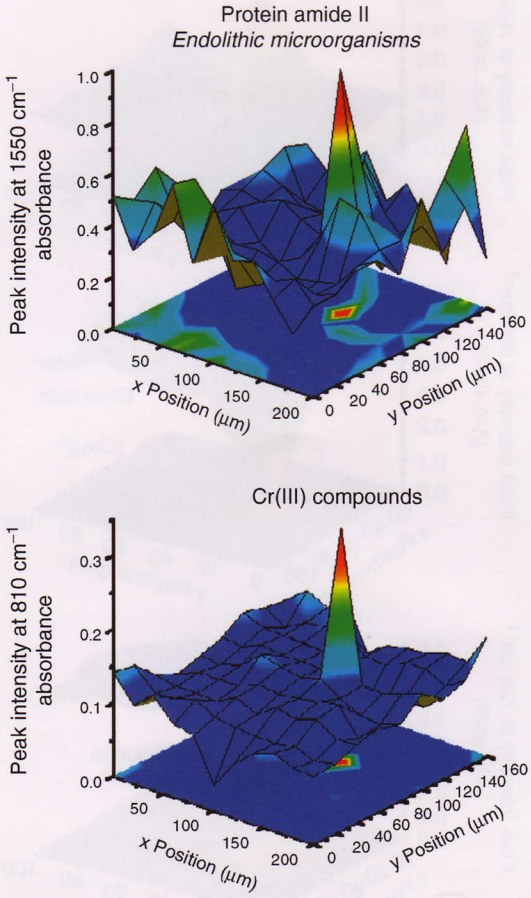

Holman and Martin, Figure 10 (See legend in text.)

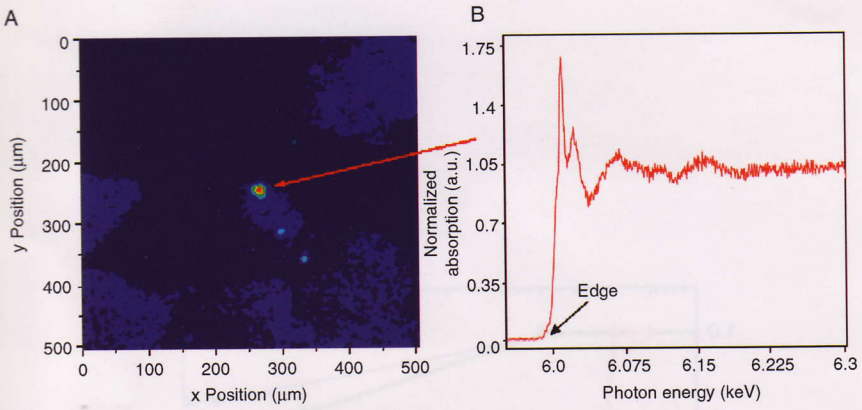

Holman and Martin, Figure 11 (See legend in text.)

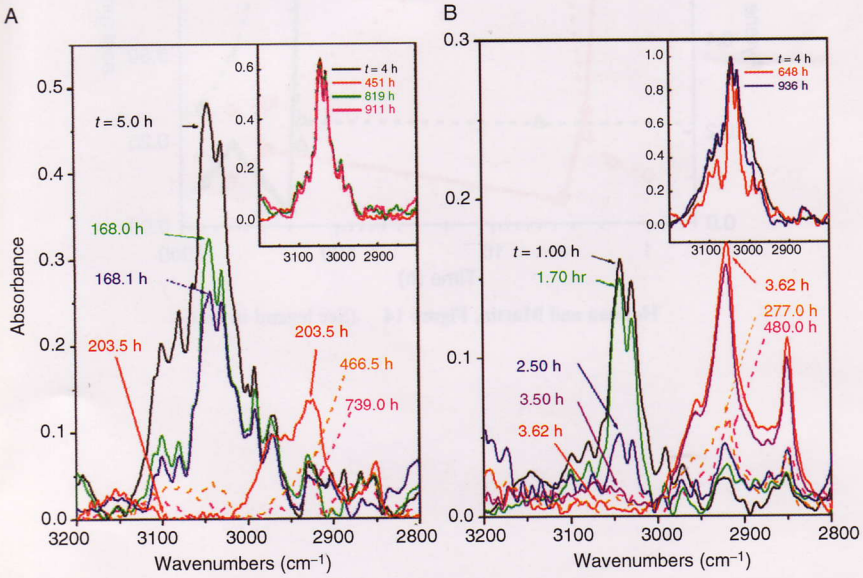

Holman and Martin, Figure 13 (See legend in text.)

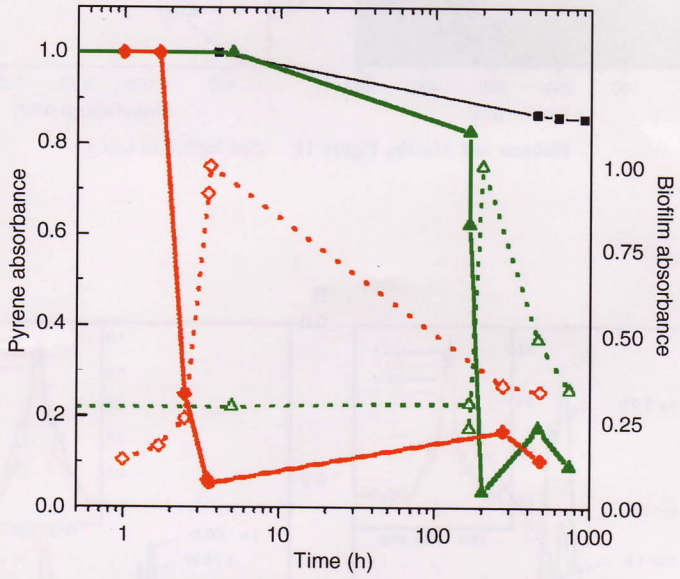

Holman and Martin, Figure 14 (See legend in text.)

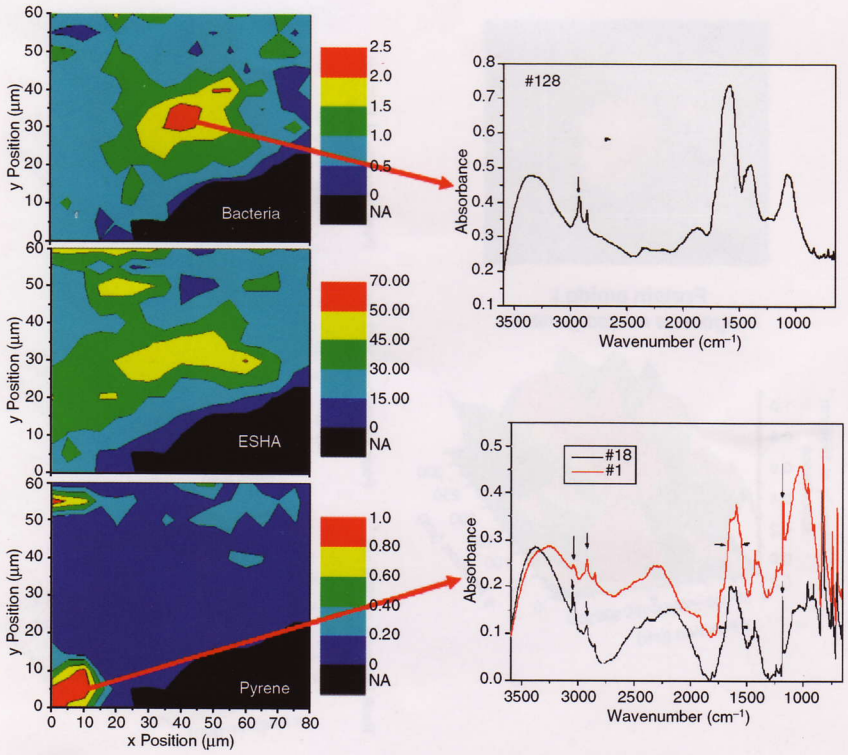

Holman and Martin, Figure 15 (See legend in text.)

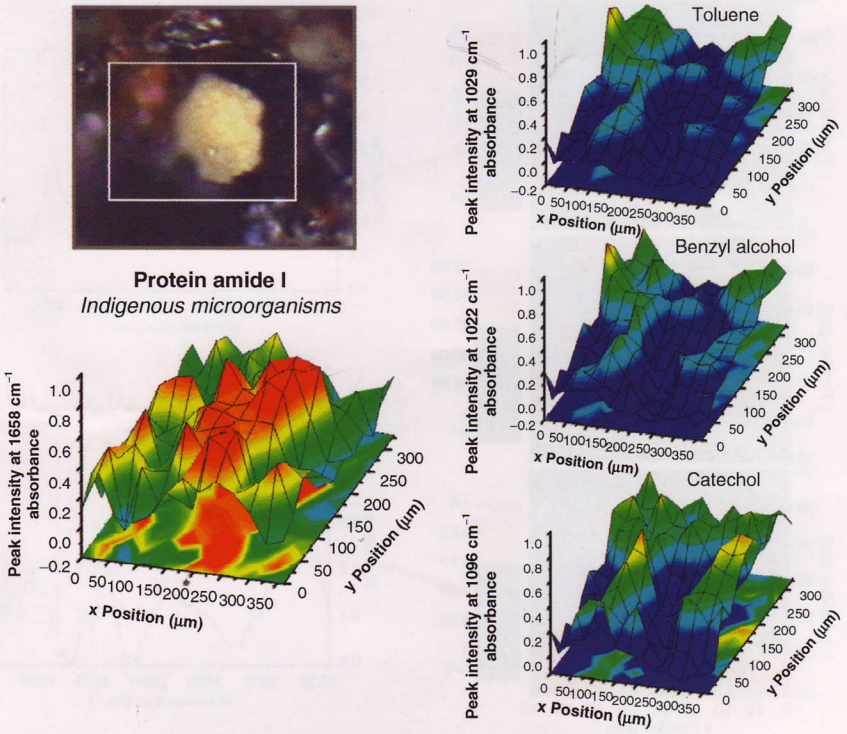

Holman and Martin, Figure 17 (See legend in text.)